

NOLTR 67-94

AD 662404

THE EARLY OPTICAL SPECTRUM AND
AIRSHOCK FROM A 500-TON TNT
EXPLOSION
(Project 1.14 of Operation SNOW BALL)

NOL

5 OCTOBER 1967

UNITED STATES NAVAL ORDNANCE LABORATORY, WHITE OAK, MARYLAND

NOLTR 67-94

D D C
RECEIVED
DEC 13 1967
RECEIVED
C

Distribution of this document is unlimited.

Reproduced by the
CLEARINGHOUSE
for Federal Scientific & Technical
Information Springfield Va 22151

THE EARLY OPTICAL SPECTRUM AND AIRSHOCK FROM A 500-TON TNT EXPLOSION
(Project 1.14 of Operation SNOW BALL)

Prepared by:
L. Rudlin
J. G. Connor, Jr.
and
John Wisotski
Denver Research Institute

ABSTRACT: Three photographic records were obtained by Project 1.14 on SNOW BALL: two millisecond framing-camera films of the explosion and one streak film of the optical spectrum.

From these records (and others from small charges) we have:

- (1) deduced that the explosion light was produced largely by impurity radiation - from sodium, calcium, and cyanogen - and by forbidden O_2 -bands; expected airshock radiation was not detected;
- (2) derived airshock pressures in the region, roughly, 5000 to 200 psi.

These derived pressures are about a factor of 2 higher than pressure-gage values. Possible explanations for this discrepancy are discussed - including the possibility that the airshock and the luminosity front were not well coupled - but no satisfactory explanation has been found.

Air/Ground Explosions Division
Explosions Research Department
U. S. NAVAL ORDNANCE LABORATORY
White Oak, Silver Spring, Maryland

NOLTR 67-94

5 October 1967

THE EARLY OPTICAL SPECTRUM AND AIRSHOCK FROM A 500-TON TNT EXPLOSION

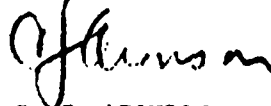
This study reports all information obtained on Operation SNOW BALL by Project 1.14 (Early Explosion Phenomenology Measurements), along with certain information from the later Operation SAILOR HAT that was necessary for interpretation of the SNOW BALL data.

Project 1.14 was conducted by this Laboratory (L. Rudlin, Project Officer) with the Denver Research Institute as contractor for the experimental field measurements (John Wisotski, Field Project Officer).

Trademarked items are named in this report solely for purposes of identification and neither criticism nor endorsement of those products is implied.

Funds for this investigation were provided by the Defense Atomic Support Agency, in conjunction with DASA NWER Subtask 01.002 (Laboratory Studies of High Altitude Explosions Phenomenology - NOL-907).

E. F. SCHREITER
Captain, USN
Commander



C. J. ARONSON
By direction

THE EARLY OPTICAL SPECTRUM AND AIRSHOCK FROM A 500-TON TNT EXPLOSION
(Project 1.14 of Operation SNOW BALL)

Prepared by:
L. Rudlin
J. G. Connor, Jr.
and
John Wisotski
Denver Research Institute

ABSTRACT: Three photographic records were obtained by Project 1.14 on SNOW BALL: two millisecond framing-camera films of the explosion and one streak film of the optical spectrum.

From these records (and others from small charges) we have:

- (1) deduced that the explosion light was produced largely by impurity radiation - from sodium, calcium, and cyanogen - and by forbidden O_2 -bands; expected airshock radiation was not detected;
- (2) derived airshock pressures in the region, roughly, 5000 to 200 psi.

These derived pressures are about a factor of 2 higher than pressure-gage values. Possible explanations for this discrepancy are discussed - including the possibility that the airshock and the luminosity front were not well coupled - but no satisfactory explanation has been found.

Air/Ground Explosions Division
Explosions Research Department
U. S. NAVAL ORDNANCE LABORATORY
White Oak, Silver Spring, Maryland

NOLTR 67-94

5 October 1967

THE EARLY OPTICAL SPECTRUM AND AIRSHOCK FROM A 500-TON TNT EXPLOSION

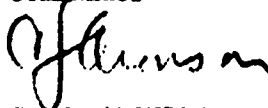
This study reports all information obtained on Operation SNOW BALL by Project 1.14 (Early Explosion Phenomenology Measurements), along with certain information from the later Operation SAILOR HAT that was necessary for interpretation of the SNOW BALL data.

Project 1.14 was conducted by this Laboratory (L. Rudlin, Project Officer) with the Denver Research Institute as contractor for the experimental field measurements (John Wisotski, Field Project Officer).

Trademarked items are named in this report solely for purposes of identification and neither criticism nor endorsement of those products is implied.

Funds for this investigation were provided by the Defense Atomic Support Agency, in conjunction with DASA NWER Subtask 01.002 (Laboratory Studies of High Altitude Explosions Phenomenology - NOL-907).

E. F. SCHREITER
Captain, USN
Commander



C. J. ARONSON
By direction

NOLTR 67-94

CONTENTS

	Page
1. INTRODUCTION.....	1
1.1 Background.....	1
1.2 Scope of this Report.....	3
2. EXPERIMENTAL DESIGN.....	4
2.1 The Charge.....	4
2.2 Instrument Stations.....	4
2.3 Instrumentation.....	4
2.3.1 Photographic.....	4
2.3.2 Electronic.....	5
2.3.3 Photographic and Spectrographic Unit Control.....	5
2.3.4 Dynafax Camera Control.....	6
2.3.5 Four-Beam Oscilloscope Control.....	6
2.4 Records Obtained....	7
3. RESULTS.....	8
3.1 Optical Spectrum.....	8
3.1.1 The Ciné-Spectrograph.....	8
3.1.2 Calibration.....	8
3.1.3 The Spectral Record.....	8
3.1.4 Identification of Spectral Features.....	10
3.1.5 Comparisons with Small-Charge Spectra.....	13
3.1.6 Canadian Measurements.....	16
3.1.7 Second-Shock Brightening.....	18
3.2 Pressure-Distance Curves.....	22
3.2.1 SNOW BALL.....	22
3.2.2 SAILOR HAT.....	24
3.2.3 Pressure-Distance Comparisons.....	25
4. DISCUSSION.....	28
4.1 Radiation Measurements.....	28
4.2 Pressure Measurements.....	28
5. REFERENCES.....	32
APPENDIX 1 - Procedure Used for Computing Pressure-Distance Curves from Radius-Time Data.....	1-1
APPENDIX 2 - Corrections for Time in Radius-Time Data.....	2-1

CONTENTS (Cont'd)

ILLUSTRATIONS

Figure	Title
1	SNOW BALL Charge in Position for Firing - Charge Radius ~ 17 Feet
2a	Block Diagram of Timing Sequence for High Speed Cameras and Ciné-Spectrographs
2b	Block Diagrams of Timing Sequence for Four-Beam Oscilloscopes and Dynafax Cameras
3	Streak Spectrum of SNOW BALL
4	Enlargement of the First Millisecond of SNOW BALL Spectrum
5	Comparison of Densitometer Tracings of Streak Spectrum from SNOW BALL and from Typical 8-Lb TNT Sphere
6	Streak Ciné-Spectrograph Image Density Resulting from Viewing 6000°K Blackbody Source
7	Comparison of Millisecond Spectra from Small TNT Spheres
8	Comparison of μ Sec Spectra from Various TNT Charges
9	Explosion Light Vs Time (1-Lb Pentolite Spheres)
10	Explosion Light Vs Time (8-Lb Pentolite Spheres)
11	Comparison of Explosion Light from SNOW BALL and from a Small Charge
12a	SNOW BALL Motion at 2611 FPS on XR Film
12b	SNOW BALL Motion at 2611 FPS on XR Film
12c	SNOW BALL Motion at 2611 FPS on XR Film
12d	SNOW BALL Motion at 2611 FPS on XR Film
13	SNOW BALL Radius-Time Growth
14	SNOW BALL Velocity-Distance Curves
15	500-Ton Hemisphere Radius-Time Curves (Spec: $T_0=6$)
16	500-Ton TNT Hemisphere Pressure-Distance Curves (Spec: $T_0=6$)
17	Comparison of Airblast Pressures from Various Multiton Charges with Computed Values
1-1	Comparison of Spec P-R Curves with Small Charge Curve
1-2	Comparison of Spec P-R Curves with Small Charge Curve from R ~ 1.5 to 14 Charge Radii
1-3	Average Deviations in Spec Fits to SNOW BALL Radius-Time Data
2-1	Comparison of Fitted Spec Curve with Film Data (SNOW BALL XR Film)

TABLES

Table	Title	Page
1	Identification of Spectral Features	10a
2	μ sec Measurements on 8-, 32-, and 100-Lb TNT Spheres	14
3	Times in Millisec for Various Amplitudes to Occur	17

1. INTRODUCTION

1.1 Background:

Our explorations of the early airshock from a small hemispherical charge suggested that the detonation wave within the explosive was transmitted into the air (RUDLIN - 1962*). This transmitted wave, thus, became the first shock created by the explosion in the outside air.

This model does not agree with the classical picture of a chemical explosion, in which the role of the detonation wave is simply to release explosive energy, the subsequent expansion of which forms an airshock.

In a later group of experiments we varied the explosive density of TNT spheres so that the strength (and other parameters) of the transmitted shock could be varied (RUDLIN - 1963). We then looked for the variations in the airshock pressures at large distances from the charges. We found no variations in these pressures that could be correlated with the charge density and thereby with the existence of transmitted airshocks. To the contrary, the airshock pressures appeared to form an unusually well-behaved group of data.

Our indirect experiments on the transmitted shock - pressure measurements at large distances away - were, thus, of little use and we were forced to perform experiments within a few charge radii of an explosion. To this end a contract to perform the experiments was awarded to the Denver Research Institute of the University of Denver. At the DRI test site we could fire charges larger than were allowed at the Naval Ordnance Laboratory. Laboratory instrumentation - μ second and millisecond cameras, spectrosopes, photomultipliers, pressure gages, etc. - was installed at the field site, and a variety of experiments have been performed with charges of size from 0.5 to 100 lbs and of different explosive materials, such as TNT, pentolite, Comp B, and PETN.

Perhaps the most important result of these DRI experiments was that we learned of a number of new phenomena that served to complicate matters. At the present time, we do not yet have a clear picture of the close-in events occurring in an explosion. There are many inconsistencies and uncertainties that we have not been able to clarify.

During the course of these small-charge experiments at DRI, we placed particular emphasis on obtaining optical spectra of the light created during the

* References are listed alphabetically in Section 5, REFERENCES.

early motion of the explosions. We wanted μ second-resolved spectra of high quality, over at least the visible part of the spectrum. Such spectra would have permitted us to see if the light that is observed on explosions is created by the shocked air - as we assumed was true (cf. RUDLIN - 1962).

If shocked-air radiation could be detected and followed in time, we could not only verify the identity of the source for explosion light but also use such spectra for estimates of shock properties. These estimates were badly needed because a number of difficulties arose in our pressure-gage measurements within a charge radius, or so, of small-charge explosions.

Participation in Operation SNOW BALL offered us an opportunity to make explorations close-in to an explosion with certain desirable advantages. The large size - 500 tons - would give us an increased time-scale for hydrodynamic phenomena - an increase of about 50 over the time-scale of our customary 8-lb charges. Further, we had estimated that SNOW BALL would give an increase of about 200 in light intensity over our 8-lb charges. Since we were having a number of problems making satisfactory μ second spectra on our 8-lb charges, we hoped that the increased time and intensity of a 500-ton shot would provide better spectra. We estimated that we had to use explosions in the multiton size to gain any substantial advantages over our 8-lb size.

Accordingly, we planned to transport much of our 8-lb charge instrumentation (cf. Section 2) directly from the Denver site to the Suffield Experimental Station (SES) site for SNOW BALL. No new instrumentation was built for the 500-ton shot. Because spectra alone would not be interpretable, we planned an integrated experiment on close-in phenomena from SNOW BALL, using cameras and pressure gages to aid in the spectral interpretation. We anticipated that differences would exist between the phenomena from small homogeneous spheres and from the rectangular-block build-up that formed the 500-ton hemispherical charge.

Our specific objectives in SNOW BALL, thus were:

- (1) to obtain experimental measurements of the explosion phenomena from SNOW BALL during early time (milliseconds); and
- (2) by comparison of these SNOW BALL measurements with similar measurements, of lesser quality, on small charges to gain a better understanding of small-charge behavior during early time (microseconds).

1.2 Scope of this Report:

Most of our instrumentation on SNOW BALL failed to provide data. Primarily, this occurred because instruments were not properly turned on at zero time.

Only three films were obtained: two millisecond framing-camera films of the explosion and one streak spectrogram. We report here our analysis of these films.

As it has turned out, we received little help from our SNOW BALL films in solving our small-charge problems. To the contrary, we have had to use μ second spectra of small charges, obtained after the 500-ton event, to interpret the SNOW BALL spectral record.

The early-time data from two films of the SNOW BALL explosion were significantly different from previous small-charge data. Our usual computer programs for explosion-motion analysis could not be used satisfactorily and a new analysis program had to be developed to accommodate the SNOW BALL films (cf. Appendices 1 and 2).

We discuss in this report (1) our interpretation of the single SNOW BALL millisecond-resolution spectral record and (2) the derived pressure-distance history of the SNOW BALL airshock during the earliest few milliseconds of motion. Much of the spectrum interpretation is necessarily based on our μ second spectral records from 8-lb charges, which we have not yet reported. We hope to report these small-charge spectral results at an early date.

2. EXPERIMENTAL DESIGN

2.1 The Charge: A close-up view of the SNOW BALL hemisphere is given in Figure 1. The charge was made up from 32.6-lb rectangular blocks, approximately 12 x 12 x 4 inches, of cast TNT. The variation in color of the blocks that appears in the photograph is real. The raw TNT came principally from U. S. (300 tons) and U.K. sources. The U. S. TNT block color was a light caramel; the U.K. TNT blocks, dark caramel. A small percentage of the blocks (~ 5 tons) were made from Canadian TNT of intermediate color. Blocks were supposedly randomly placed in building up the charge with no regard to origin of the TNT. But, as we note in Figure 1 and especially so in other views of the charge, there was a heavier concentration of U.K. blocks in the surface of the upper third of the charge. The radius of the charge, a_0 , was approximately 17 feet.

2.2 Instrument Stations: Primarily, instrumentation was optical. Our instrument station was located along the 296° line at 3400 feet in the Canadian sector near Canadian B bunker. Various cameras and spectrographs were located directly on the ground or on tables. Personnel were accommodated in B bunker to turn on equipment and to operate the control panel during the shot. Pressure-time gages were located at 2, 3, 7, and 10 a_0 with hard-wire control from B bunker.

2.3 Instrumentation:

2.3.1 Photographic:

a. Ciné-Spectrographs*

(1) Streak: nominal 100 ft/sec, 70 mm Tri-X film

(2) Framing: nominal 4000 fps, 70 mm Tri-X film

b. Cameras

(1) Fairchild: nominal 5000 fps; 76 mm f/11 lens with superposed Balzer red filter; 16 mm ER Ektachrome film

(2) Eastman High Speed: nominal 2500 fps; 63 mm f/2 lens; 16 mm XR film

* We are indebted to Dr. P. A. Tate, DCBRL, Ottawa, for making the Ciné-Spectrographs available to us.

- (3) Fastax: nominal 5000 fps; 50 mm f/8 lens with superposed Wratten 87 filter; 16 mm Eastman High Speed Infrared film
- (4) Dynafax: nominal 25,000 fps; 75 mm f/3.5 lens with 1 μ sec diamond stops; 35 mm ER Ektachrome film
- (5) Dynafax: nominal 25,000 fps; 75 mm f/3.5 lens with 1 μ sec diamond stops and superposed Balzer blue filter; 35 mm ER Ektachrome film

2.3.2 Electronic:

a. Four-Beam Oscilloscopes (2 millisc/cm)

- (1) Scope A
 - (a) Photomultiplier, 931A, with Balzer blue filter
 - (b) Photomultiplier, 1P22, with Balzer blue filter
 - (c) Photomultiplier, 931A
 - (d) Solar Cell, SPR 5-08, with Balzer red filter
- (2) Scope B
 - (a) Photomultiplier, 1P22
 - (b) Solar Cell, SPR 5-08
 - (c) Two P-t (40 $\mu\mu$ coulombs per psi) Gages connected in parallel at 3 and 10 charge radii
 - (d) Two P-t (40 $\mu\mu$ coulombs per psi) Gages connected in parallel at 2 and 7 charge radii
- (3) Drum Camera (12.5 mm/millisc) using 70 mm Tri-X film (50 inches long)

2.3.3 Photographic and Spectrographic Unit Control: Five photographic and spectrographic units were controlled by a relay closure in the Multiple Relay Station supplied by the Suffield Experimental Station Central Control. This closure occurred at approximately -2.3 seconds before Console Zero (-6 \pm 2 millisc). This signal started the event sequence of the Sequence Timer Unit supplied by DRI. This unit gave the necessary lead-time to the high speed cameras and the Ciné-Spectrographs. The lead-times were predetermined for each unit so as to allow the

event to be recorded after more than 50 feet of the film had been run. This allowed the units to obtain close to maximum speed permitted by the power-supply generators. The three high-speed cameras were powered by separate 2.5KVA generators, situated approximately 50 feet from the camera stations. The Ciné-Spectrographs were powered by one 220 VAC, 10 KVA generator, situated approximately 250 feet away from the spectrograph stations. The power to these units was supplied over three-wire No. 4 cable which was rated at 70 amperes.

The film speeds were obtained by using timing-light generators located near the camera stations. A timing-light generator was not used for the Fastax camera since it contained infrared film. The Ciné-Spectrographs had self-contained timing-light generators.

The lead-time for each unit triggered by the Sequence-Timer is given in Figure 2a.

2.3.4 Dynafax Camera Control: From the Multiple Relay Station we obtained another relay closure signal for triggering the two Dynafax cameras shutters (see Fig. 2b). The console zero signal (-6 ± 2 millisecc) gave ample lead-time for opening the Dynafax cameras shutters, since they were being energized by a relatively high-voltage, high-capacity source (90 volts at 800 microfarads). The switching of the 90 VDC was accomplished by using a silicone-controlled rectifier (gate-control rectifier), triggered by a signal from a transistorized multivibrator circuit.

The Dynafax shutter was set to close 13 millisecc after the console-zero signal. This setting would allow the recording of a minimum of 4 millisecc or a maximum of 8 millisecc of the event - depending on whether the console zero signal was actually -4 or -8 millisecc before detonation zero. One millisecc was assumed to be the time for first light to appear after detonation zero. With a recording time of 8 millisecc, a total of 244 frames would have been recorded. The speeds of the Dynafax cameras were controlled remotely in B bunker by using two Variacs and a millisecond period counter.

2.3.5 Four-Beam Oscilloscope Control: The two four-beam oscilloscopes were used to record pressure-time and photoelectric signals on 50 inches of 70 mm film. The film record was to have been made on a drum camera rotating at a speed of 500 inches per second, giving a one-revolution recording time of 100 millisecc. The event-time was controlled by the two four-beam oscilloscopes which were set at

2 millisecc/cm, thus giving a total recording time of 200 millisecc. With the speed of the drum camera set for 100 millisecc/rev, the total 200 millisecc of the event was recorded by rewinding the trace one time. The oscilloscopes were triggered by a console zero signal through a transistorized one-shot multivibrator circuit which responds rapidly to a switch closure type of signal (see Fig. 2b).

The two oscilloscopes were placed side by side so that the drum camera could simultaneously record both sets of four beams by observing them with a first-surface beam-splitting mirror. The shutter on the camera was opened manually, prior to the sequence of events. Although the two oscilloscopes and the beam-splitting hardware were fairly well sealed from ambient light, all the equipment in the bunker was run in darkness to insure a minimum of leakage during the detonation. The photoelectric devices were coupled directly through coaxial cables (21-467) into the channel amplifiers of the oscilloscopes, whereas the pressure-time gages were coupled through coaxial cables (21-467) into high input impedance Keithley amplifiers before the signals were coupled to the channel amplifiers of the oscilloscopes.

2.4 Records Obtained: Useable records were obtained only from three instruments:

- a. Fairchild - 3817 fps, radius-time data useable for 10 millisecc; Balzer red filter (peak light transmission at 6500 Å with 40 per cent transmission at 6150 and 6700 Å), used over ER Ektachrome film.
- b. Eastman - 2611 fps, radius-time data useable for 25 millisecc on XR film.
- c. Ciné-Spectrograph - streak at ~ 25 mm/millisecc; spectral range from about 2900 to 7000 Å for 120 millisecc; slit size: 51 μ by 5 mm, leading to time resolution of about 0.2 millisecc.

3. RESULTS

3.1 Optical Spectrum:

3.1.1 The Cine-Spectrograph: This instrument is of the moving-film type,* with a peak speed of about 30 m/sec. As designed, the spectral region from 2500 to 8000 Å is dispersed over 40 mm of the width of 70 mm film. Along the length timing markers are placed during use at a rate of 1 mark/millisecond. Dispersion varies from about 40 Å/mm (at 2700 Å) to about 600 Å/mm (at 6000 Å).

3.1.2 Calibration: No attempt was made to calibrate the instrument for intensity, our main interest being a qualitative estimate of the spectral output of the explosion. To meet these needs, however, a wavelength scale was placed on the film of the spectrograph, in situ, before the explosion by use of a known mercury-line spectrum. Because the intensity of the mercury source was far below that of the explosion, the spectrograph was not run at full speed when the calibration was superimposed on the film.

We later found, during the analysis of the film, that the calibration lines were not reliable. At full speed the film moves an excessively large distance in position as it slips along the sprocket holes. Accordingly, we did not use the mercury lines for identification, but instead used certain lines on the SNOW BALL explosion spectrum that we later identified from small-charge spectra.

3.1.3 The Spectral Record: In Figure 3 we see a portion of the 120 millisecond record obtained. At the beginning of the record we note that all wavelengths do not appear to begin at the same time. The time resolution of this instrument is determined by the height of the slit. As used on SNOW BALL, this was ~ 200 μsec or 1/5 of the distance between markers. Any light, of sufficient intensity to record on the film, that occurred within zero to + 200 μsec should have been recorded on the film. The record could be interpreted to suggest that various wavelengths might have started radiating at different times. But we rather believe that the less intense light in the blue part of the spectrum was not sufficient to record.

* The basic instrument has been described by Lovell, Stewart and Rosen, "Ciné-Spectrograph," J. Opt. Soc. Am. 44, 799, 1954. The instruments used were of Canadian design and manufacture and differ from the earlier instruments in some details.

A number of lines and bands appear in the earliest part of the record (cf. enlargement of Figure 4). Most of these spectral features become lost in the apparent continuum at later times. As time advances most of this continuum dies out, leaving only a small image at the red end of the spectrum. This image continues, unchanged, out to about 120 millisecc before disappearing from the record. The longest-lived spectral feature is the sodium doublet (at 5890 and 5896 Å but not resolved on the spectral film) which persists to about 65 millisecc before disappearing from the record.

Whether or not real continuum radiation exists on this record is not clear. Inspection of similar small-charge records suggests that over exposure of the many lines and bands could produce what appears to be continuum radiation on the film.

We can examine this, although we cannot reach any definite conclusions. In Figure 5 we have compared the tracings produced by a densitometer traversing the streak spectrum from SNOW BALL and from a small charge at a fixed time. For both tracings an arbitrary time was selected shortly after an image was produced on the film; the same time position was used on both films. Intensity was merely roughly matched for both records at the red end of the spectrum. There are obvious similarities in the peaks on both tracings and a somewhat less obvious similarity in the shapes of the curves.

The Ciné-Spectrograph is a prism device and we have accounted neither for its non-linear response nor for the non-linear response of the film in Figure 5. In Figure 6 we have attempted to estimate how the film and the prism modify a 6000°K blackbody spectrum.* The radiation from the theoretical source was analytically passed through the dispersion curve of the spectrograph prism (as experimentally determined) to make the lowest curve in Figure 6, labeled "perfect film." As we could have expected, the prism crowds up the energy at the red end of the perfect film.

To estimate what happens with real film, the (nominal) spectral-response characteristics of two films that we have commonly used in the Ciné-Spectrograph

* We do not want to suggest that an explosion radiates like a 6000°K blackbody.

We intend this source value merely for illustrative purposes. Any other source function would do as well.

were accounted for. The upper curve, labeled Tri-X, gives the estimated image density that a 6000°K blackbody would produce on Tri-X film in our particular spectrograph. The dip, at about 5000 Å, results from the decrease in film sensitivity in this part of the spectrum. (Both spectral records shown in Figure 5 were made on Tri-X film.)

The image density on Shellburst film is also drawn in Figure 6 to indicate what variations might occur on another type of film. There is no relation whatsoever from one curve to another in Figure 6; these curves were grouped on the graph only for convenient viewing. Along a given curve, however, relative intensity is correct.

Returning to Figure 5, we can note a general resemblance of the explosion spectral tracings with the 6000°K blackbody response on Tri-X film. But there are a number of questions to be answered before we could conclude that the explosion light corresponds to blackbody radiation with superposed lines and bands; and we do not so conclude.*

3.1.4 Identification of Spectral Features: There are only a few easily recognizable spectral features in the SNOW BALL record. We have had to use our unreported small-charge spectra both to find and to identify lines and bands in the SNOW BALL record. We list in Table 1 the features that we believe exist in SNOW BALL and in a typical small charge (8-lb TNT) explosion.

For the small charge two kinds of spectra were available: (1) the Ciné-Spectrograph record (as for SNOW BALL) and (2) a Hilger record without time resolution. The Hilger was left open during the entire explosion, which partly accounts for the absorption lines on this record. Both records were obtained from the same explosion - so that the presence of features on one record but not on another in Table 1 gives a hint of some of the problems in finding spectral features on explosions records.

The same type of film (Tri-X) was used for all records in Table 1. The red end of the records was cut off by the lack of film response. At the blue end, both Hilger and Ciné-Spectrograph should have been able to go down to about 2500 Å. The Ciné-Spectrograph on the small charge probably did not have a large

* μ second spectra from small non-TNT charges would suggest that explosion light is not blackbody continuum. That such records from small TNT charges (and from SNOW BALL) resembles blackbody radiation may be purely an accident.

TABLE 1 IDENTIFICATION OF SPECTRAL FEATURES

SNOW BALL (Å)	B-LB CHARGE			IDENTIFICATION			SNOW BALL (Å)	B-LB CHARGE			IDENTIFICATION		
	HILGER (Å)	CINE (Å)	WAVE. (Å)	SPECIES	INTENSITY	HILGER (Å)		CINE (Å)	WAVE. (Å)	SPECIES	INTENSITY		
2825				?		3715				?			
2830			2850	O ₂ - H	5	3725		3726	O ₂ - BG	?			
2875			2870	O ₂ - SR	7	3733		3734	O ₂ - H	?			
2895			2895	O ₂ - H	6	3743*		3737	O ₂ - BG	?			
2925			2923	O ₂ - SR	7	3757*		3754	NIGHT-SKY	?			
2947			2945	O ₂ - H	5	3795		3793	O ₂ - BG	?			
2975			2984	O ₂ - SR	8	3825		3827	O ₂ - BG	?			
2990				?				3829	O ₂ - H	?			
3003			3002	O ₂ - H	5	3847		3840	O ₂ - SR	8			
3025			3026	O ₂ - H	3			3840	CN VIOLET	6			
3045			3066	O ₂ - H	5	3865		3854	CN VIOLET	8			
3080			3080	O ₂ - H	7	3875		3871	CN VIOLET	9			
3100			3093	O ₂ - SR	5	3883		3883	CN VIOLET	10			
3105			3104	O ₂ - SR	8								
3115						3915							
3125													
3145			3142	O ₂ - H	7	3923		3924	Ce	?			
3155			315*	NIGHT-SKY	?	3940*		3948	NIGHT-SKY	?			
3170			3171	O ₂ - H	?	3960		3968	Ce	?			
3210			3211	O ₂ - H	10	3970		3972	O ₂ - BG	?			
3225			3232	O ₂ - SR	9	3975*							
3245				?									
3297			3285	O ₂ - H	7			4018	NIGHT-SKY	?			
			3365	O ₂ - BG	7			4032	O ₂ - BG	?			
3370			3375	O ₂ - H (110) OR POSSIBLY NH (1, -1)	?	4030		4043	O ₂ - BG	?			
				O ₂ - BG	?	3970		4096	O ₂ - SR	5			
3415				?		4070		4117	NIGHT-SKY	?			
3447			3453	O ₂ - H	8			4155	NIGHT-SKY	?			
			3456	O ₂ - BG	?			4158-67	CN VIOLET	5-6			
			3465*	O ₂ - BG	?			4180	CN VIOLET	7			
3470			3480*	O ₂ - H	?			4195	CN VIOLET	8			
			3483*	O ₂ - H	?			4227	Ce	?			
			3505*	?				4310*	O ₂ - H	7			
3520			3520*	O ₂ - SR	10			4565	O ₂ - H	5			
3540			3540*	O ₂ - H	8			4835	O ₂ - BG	?			
3570			3567	O ₂ - H	?			5160	NIGHT-SKY OR POSSIBLY NO ₂ SR	?			
				?		3915		?					
3590			3584	NIGHT-SKY	7	5590		5890-96	N ₂ D				
			3590	CN	8	5893							
3635			3625*	O ₂ - BG	?								
			3633*	O ₂ - H	8								
3640			3638	NIGHT-SKY	?								
			3657*	O ₂ - BG	7								
3670			3671	O ₂ - SR	9								

NOTES

- *SEEN ONLY IN ABSORPTION
- O₂ - B BAND (PRESUMABLY OXYGEN) OF NIGHT-SKY GIVEN BY BARBIER, ANNI, DE GEOPHYS., 1, 224, 1945.
- O₂ - BG OXYGEN BAND CALCULATED BY BROIDA AND GAYDON, PRO. ROY. SOC. 222, 181, 1954.
- O₂ - H OXYGEN BAND GIVEN BY GAYDON, THE IDENTIFICATION OF MOLECULAR SPECTRA, JOHN WILEY & SONS, INC., 1963
- HERZBERG FORBIDDEN TRANSITION A ³Σ_g⁻ - X ³Σ_g⁻
- O₂ - H HERZBERG OXYGEN BAND GIVEN BY CHAMBERLAIN, ASTROPHYS. J., 121, 277, 1955.
- O₂ - SR OXYGEN BAND GIVEN BY GAYDON, THE IDENTIFICATION OF MOLECULAR SPECTRA, JOHN WILEY & SONS, INC., 1963
- SCHUMANN-RUNGE TRANSITION B ³Σ_g⁻ - X ³Σ_g⁻
- NIGHT-SKY BANDS (PROBABLY OXYGEN) OF NIGHT-SKY GIVEN BY CABANNES DUFAY, ANNI, DE GEOPHYS., 2, 290, 1946.

enough volume of light to record on the film. (We are not sure why the Hilger, with a larger f-number than that of the Cine-Spectrograph, recorded deeper into the blue. Possibly this resulted from the slightly longer exposure time of a grain of emulsion on the Hilger film where the film was stationary.)

Confidence in the identifications made in Table 1 varies considerably.

- (1) We are quite confident that the lines at 5893 and 4227 Å are Na and Ca. These have been seen both in emission and in absorption in small-charge tests under a variety of circumstances.
- (2) We are only slightly less confident that the bands at 3590, 3863, and 4197 Å belong to the CN-violet system. Although the circumstantial evidence for these is not so positive as for Na and Ca, wavelength separation and intensity values of the members of the individual bands agree.
- (3) We are less confident of our identification of the forbidden- O_2 transitions (such as $O_2 - H$, and $O_2 - BG$) of Table 1. We were first able to identify these from manipulated enlargements of the film. They could not be detected with a traveling microscope or a densitometer on the film. To check the reality of the lines barely detectable in the enlargements, densitometer tracings were made of the prints. Agreement of a densitometer peak and an appearance of a line on the print was good. We were somewhat surprised to find that we could tally every band head (of intensity 5 and over) given by Gaydon for the Herzberg system* with a SNOW BALL line with one exception (out of about 20 possibilities). Such correlation could be accidental. With this O_2 -Herzberg identification made only on one (the SNOW BALL) record, we cannot be sure.
- (4) We are next least confident of the O_2 bands and night sky bands of Table 1. These bands can be readily found on our small-charge explosion records. We have not been able to tie them to any species that we might expect to find - such as, for example, CH, NH_2 , OH, or possible explosion products. If the O_2 -Herzberg identification is correct, as we think it is, then we should expect other low-energy forbidden systems of oxygen to be present.

* Labeled O_2-H in Table 1.

- (5) We are least confident of the O_2 Schumann-Runge identifications. These were obtained not by finding the lines first but by looking for the existence of lines at wavelengths where O_2 - SR of intensity 5 or greater might be present. Gaydon lists some 15 such SR values from 2870 to 4179 Å. We can identify peaks on the densitometer tracing of the SNOW BALL enlargements for all 15 wavelengths (although several of these we have preferred to tie to a species other than O_2 - SR).

Perhaps more surprising than what we have identified in the SNOW BALL spectrum is what we have not found. Not only have we found no evidence of any of a number of possible explosion products, but also we see no evidence of shocked-air spectral features.* We have not found any evidence of NO_2 absorption on the spectrum. The formation of NO_2 at the shockfront from an explosion has often been postulated to explain the intensity-time behavior of light from an explosion.**

The excitation energies of the species that we do identify in Table 1 are all low. The O_2 -Herzberg system, for example, requires about 1.7 ev. Substantially more excitation energy is needed for the O_2 -Schumann Runge system (about 6.2 ev). Without attempting to account for the energetics involved in producing light from an explosion, we are not too startled to find that only low-energy excitations are created by an explosion and not the considerably higher energy radiations theoretically predicted for shocked air.

* Theoretical estimates vary on what should be seen from shocked air. Allen gives a number of recent estimates for various nitrogen and oxygen radiators. We hope to discuss this more fully at a later date when we will report our small-charge spectra. These spectra have more detail and extend more deeply into the important near-infrared region.

** See, for example, Raizer, In.P., "Glow of Air During a Strong Explosion and the Minimum Brightness of a Fireball," Soviet Physics JETP 34, 331, 1958; or Tate, P. A. and Pattman, J. D. R., "100 Ton TNT Hemispherical Charge (1961); Project No. 4 Thermal Measurements," Defence Research Chemical Laboratories Report No. 371, June 1962.

What we can identify in the SNOW BALL spectrum, thus, leads us to conclude that much of the radiation is produced by low-energy O_2 -band transitions and "impurity" radiation, such as produced by sodium, calcium, and cyanogen. We should like to be able to pin down whether these radiators are excited in the air (say by the shock or by particles) or are excited explosion products. We cannot do so.

Examination of a small part of the literature on natural impurity radiation from air suggests to us that our sodium, calcium, and cyanogen radiation could have been produced in the air alone; clearly it could have been produced by the explosion products. The O_2 -radiation clearly could have been produced in the air alone, since such radiation is a part of the night sky spectrum. But we cannot rule out such light produced by free O_2 in the explosion products - granted that we have no evidence at all to support the presence of O_2 -Herzberg light from chemical reactions.

As reasonable a guess as any is that the impurity radiation is produced by the explosion products and the O_2 -band light is created by excited air.

3.1.5 Comparisons with Small-Charge Spectra: In Figure 7 are Ciné-Spectrograph spectra for three spherical TNT charges of 8, 32, and 100 pounds. These charges were cast from the same batch of TNT powder under presumably identical conditions. A lens was used to collect the light on all three shots.*

The rectangular appearance of the early-time part of the spectrum results from the slit height used. The slit height used for the three spectra of Figure 7 was the same and corresponded to, roughly, 100 μ seconds** on the spectra. This means that the time resolution of the Ciné-Spectrographs of Figure 7 is not better than 100 μ sec; any event, shorter than 100 μ sec, that occurred would be recorded with a duration of 100 μ sec.

We note that the red end of the spectrum seems to appear earlier than the blue end in both the small-charge spectra of Figure 7 and the SNOW BALL spectrum. Small-charge spectra taken with μ sec resolution show a similar tendency (cf. Fig. 8). However, this time separation is roughly only a few μ seconds; the

* Scaling procedures for explosion-shock light have been discussed by ERICSSON.

For convenience, charge-to-lens distances were selected for these shots so that the square of the distance was in proportion to the square root of the charge weight, based on the distance of 70 feet for the 8-lb charge.

** The slit height used on the SNOW BALL spectrum (Figs. 3 or 4) corresponds to about 200 μ sec.

separation in the SNOW BALL spectrum is probably exaggerated by overexposure at the red end of the spectrum. We do note slight differences in the times at which certain spectral features end. The CN 3590 line appears to end slightly before the CN 3883 group ends. The Ca 4227 and the Ca⁺ 3968 and 3934 appear to last slightly longer than does the CN 3883 group. The sodium doublet, centered at 5893 Å, is the longest-lived line of these spectra.

The black lines on the 8-lb spectrum of Figure 7 are scratches on the film and do not represent absorption lines. An absorption line (5893 Å) does begin on the 32-lb spectrum at roughly 0.5 millisecc.

As time increases the spectral features die out in the blue and yellow regions, continuing in the red. The Tri-X film response causes the sharp cut-off in the red at about 6400 Å.* Rough estimates of the maximum time duration can be made for the three shots of Figure 7. We find the following times when light ceases to appear on these spectra:

8-lb	0.7 millisecc
32-lb	0.8 millisecc
100-lb	1.6 millisecc

More accurate timing measurements, at early time, were made on these three shots with electronic (photodiode) gages, having a time resolution of roughly 3 to 5 μsec.** These results are given in Table 2 for measurements integrated over the range 6650-8200 Å with a peak at about 7300 Å.

Table 2

μsec Measurements on 8-, 32-, and 100-Lb TNT Spheres

Weight	Rise Time to Peak Amp. (μsec)	Decay Time to 1/2 Peak Amp. (μsec)	Peak Amp. (volts)
8 lb	12	120	2.9
32 lb	10	52	5.4
100 lb	16	50	3.6

* Other types of film that we have used have recorded explosion spectra to 9000 Å.

** These measurements, and other μsecond results on small charges, will be reported later.

These timing results are baffling and we see no clear-cut scaling from one charge weight to another. If light from the explosion were hydrodynamically produced, either by the airshock or by chemical products directly influenced by the hydrodynamic-flow parameters, then we would expect to find that cube-root scaling holds for charges of different weight. What we would expect, on this basis, is:

- (1) Irrespective of the weight of the charge, the maximum airshock pressure that can be produced by a certain chemical explosion is a constant. If we measure distance in units of, say, charge radius, then we should find that all charges (from a fixed chemical composition, etc.) produce the same pressures and all other hydrodynamics parameters at the front. The only detectable difference between charges of different size should be the time of events behind the shockfront. If the airshock produced explosion light, we should expect to see either particular species of air radiate in lines (or bands) or we should see a continuum or, possibly, we should see a mixture of both.
- (2) If we see no sign of shocked air, as we believe is the case for the TNT charges discussed in this report, then we might expect to see radiation produced by the chemical products of explosion reaction. We would think that the luminosity produced by these products depends on local values of temperature and density. These values would be determined by the airshock, presumably, ahead of the products. Clearly, then, we would expect the luminosity to depend on the cube root of the charge weight.

Our results on the 8-, 32-, and 100-lb shots do not show that cube-root scaling holds. For that matter, the dependence on charge weight looks almost haphazard. This surmise might be illustrated by the μ sec spectra of Figure 8. These spectra were made with a home-made prism spectrograph which used an AVCO streak camera, writing at ~ 1.2 mm/ μ sec, as the recorder.

Spectra b and c of Figure 8 were made on the same shots from which the millisec spectra of Figure 7 were obtained. Spectrum a was made on a block charge* cast in a manner similar to that used for the blocks of the SNOW BALL shot.

* This particular block was taken from a batch used in making the 500-ton charges for Operation SAILOR HAT.

In the original spectral films of Figure 8 there is no difficulty in recognizing differences in the three spectra. The 33-lb block charge, for instance, does not produce the higher-energy radiators, such as the CN 3883 and CN 4216 bands or Ca^+ lines at 3934 and 3968 Å that we see for the 32-lb or 100-lb spheres. The weak lines that do appear in the block spectrum appear to belong to low-energy levels for calcium, barium, and sodium (energies between 2 to 5 ev).

Also, we may note that certain radiators that appear in the 32-lb sphere spectrum do not appear in the 100-lb spectrum. For example, the CN 3883 group and the Ca^+ doublet at 3934 and 3968 Å do not appear. On the other hand, the red-end radiation on the 100-lb shot is, clearly, much stronger than is the red-end radiation on the 32-lb shot. The 5595 Å line, which is easily visible on the 32-lb spectrum, for example, is wiped out by the excessive light on the 100-lb spectrum.

The spectra of Figure 8, thus, suggest that the particular radiators excited during an explosion can vary from explosion to explosion. The two spherical charges used for b and c of Figure 8 were presumably made from the same batch of TNT powder and fired under identical conditions. The block charge (a of Fig. 8), however, was made from unknown powder under different conditions.

Most of the radiation emitted by the TNT explosion comes from the red and the deep red part of the spectrum. Our spectra of Figure 8 do not give us much information on the details in this part of the spectrum as a function of charge weight. The variations from charge to charge in the blue and yellow parts of the spectrum, suggested by the spectra of Figure 8, may well occur and yet not be of significance - since such variations contain only a small part of the total radiant energy produced by an explosion. The photodiode measurements of Table 2 in the red part of the spectrum do suggest variations from charge to charge in this region also.

Canadian measurements on SNOW BALL suggest that cube-root scaling does, indeed, hold (cf. next section). The scaling situation is far from clear.

3.1.6 Canadian Measurements: PATMAN and TATE used a variety of instruments to record the radiation produced on SNOW BALL: high-speed bolometers with broad bandpass in wavelength, photocells viewing several relatively narrow bands of the spectrum, and calorimeters. Our photodiode measurements had been planned to overlap the Canadian photocell measurements so that comparisons between the

two groups could be made. Failure of our control panel prevented our obtaining photodiode records. We will make other fragmentary comparisons in this section.

PATMAN and TATE reached several conclusions from their records, some of which we note:

- (1) The three maxima of the 500-ton thermal pulse (intensity vs. time) cube-root scaled to the maxima on the 100-ton TNT hemisphere thermal pulse. Two minima, which occur adjacent to these maxima, do not appear to cube-root scale.
- (2) Temperatures, measured by the infrared photocells, on the 500-ton and the 100-ton shots cube-root scaled in time.
- (3) The fraction of the explosion energy available (based on 10^9 calories per ton of TNT) going into radiant energy was about 5 per cent on SNOW BALL. On the 100-ton shot the comparable value was about 8 per cent. Comparable measurements on 20-ton TNT hemispheres gave the largest fraction measured - 17 per cent.

These three conclusions indicate that although there may be variations in the amount of radiation produced by an explosion, the times at which particular radiant features appear do cube-root scale. Using our 100-lb photodiode μ sec record, we can compare certain critical times (scaled up to 500 tons) with the times found by PATMAN and TATE. These times are compiled in Table 3.

Table 3

Times in Millisec for Various Amplitudes to Occur

Charge	Rise to Peak Amp.	Decay to		
		3/4 Peak Amp	1/2 Peak Amp.	1/4 Peak Amp.
100 lb	1.12	1.65	1.93	2.48
500 tons	0.97	1.33	1.53	2.13

Certain differences between the data in Table 3 must be noted. Our μ sec record covers only the time period of the first pulse seen on a millisec scale by PATMAN and TATE. There is an important difference in the way the two explosions were viewed: the 500-ton charge was always within the field of view - the entire explosion surface was seen by the photocell; a fixed field-of-view, covering only a part of the explosion surface, was used on the 100-lb shot. The times given in Table 3 refer to zero time when the detonator went off. On the 100-lb record

the detonator firing appears as a wide pulse on the 20 $\mu\text{sec}/\text{cm}$ oscilloscope record. If we assign an uncertainty of 5-10 μsec to the precise time when the detonator went off, this uncertainty would be multiplied up (by the cube root of the ratio of the charge weights) to about 0.1 to 0.3 millisecon on the 500-ton scale. With these differences in mind between the two sets of data in Table 3, we believe that the comparison indicates that cube-root scaling of amplitude-vs-time does hold between the μsec pulse of the 100-lb sphere and the millisecon pulse of the 500-ton hemisphere.

3.1.7 Second-Shock Brightening: We can make another comparison, a brightening after the first airshock, by finding the transmission of the frames of a motion-picture film as a function of time. In Figures 9 and 10 we have plotted transmission measurements from 1- and 8-lb pentolite spheres.

The precise meaning of these curves needs to be explained: these signatures represent the maximum transmission of frames of 16 mm films taken at 2500-5000 fps. Transmission of each frame was obtained by scanning a Jarrell-Ash densitometer through the center of the fireball to the outer edge of the fireball in each frame. From each frame, a maximum transmission value was determined and plotted in Figures 9 and 10 as the transmission at the time (of that frame) during the explosion. The transmission units are arbitrary readings on the densitometer.

In order to examine different wavelengths of the radiation from the explosion, we have used filters to limit the light reaching our color films. For these experiments, High-Speed Ektachrome was used as the color film; Balzer interference filters* and a Wratten C-5 filter were used to filter the light. The signatures of Figures 9 and 10 are labeled to represent which filter was used to obtain the signature.

* Tests of these filters indicated the following limits of response (zero per cent transmission):

Balzer red:	5000 \AA - ? (85 per cent transmission at 9600 \AA)
Balzer green:	4750 \AA - 7800 \AA
Balzer blue:	3540 \AA - 5520 \AA
C-5 (blue):	3740 \AA - 5200 \AA

A troublesome feature should be mentioned: both the C-5 filter and the Balzer green filter were found to open up again in the far red, reaching about 30 per cent transmission at the end of our wavelength capability at 9600 \AA .

We note that the characteristic trace shows a bright first maximum at zero time, followed by a minimum and then a second maximum. The time of the minimum and also of the second maximum does not appear to depend significantly on the wavelength band of the filter. The times do depend on the weight of the charge. We may note that for the 1-lb spheres the minimum occurred at about 1.2 millisecc; and the second maximum, at about 1.8 millisecc. The corresponding times for the 8-lb charges occur at closely twice the 1-lb values. Apparently these light phenomena follow cube-root scaling for time of occurrence.

A number of pieces of evidence indicate that the second maxima found in the intensity-time traces of Figures 9 and 10 are caused by the passage of the second shockwave through the fireball. Our evidence, admittedly, is circumstantial and no direct tests of our second-shock hypothesis have been made.

We have found that:

- (1) The time of second maximum luminosity corresponds to the time that the second shock leaves the explosion gases, as deduced from pressure-time gages and from shock photography.
- (2) The second shock produces sizeable luminosity within the fireball in explosions at an altitude of 100 kft.*
- (3) No second maxima are found for small (2.5-lb) hemispherical explosions fired in free air. We expect that the second shock will fail to propagate away from the center of a hemisphere because of the lack of spherical symmetry. Therefore, we do not expect to find a second shock moving back through the explosion fireball; and we do not find second shocks on pressure-time records of free-air hemispherical records. The tie between the existence of the second shock and the brightening on spherical explosions and the lack of this tie on hemispherical explosions appears to us as a convincing explanation for the role of the second shock as the mechanism of this phenomenon.

How the second shock produces the increase in luminosity is not yet answerable. We do not know if the second shock is itself hot enough to be

* Knodle, R. L. and Hanlon, P., "Air Blast Results for Project Banshee," U. S. Naval Ordnance Laboratory NOLTR 63-268, 12 November 1965.

luminous - or, if the second shock triggers chemical reactions, a second burning - or, if the second shock triggers radiation to be released from some forbidden states - or, if the density increase that accompanies the second shock is alone able to account for the increase in luminosity. Our attempts to obtain spectra of the second-shock light from small charges have not been successful.

On SNOW BALL we purposely exposed Ektachrome film through a red filter to obtain a film similar to those obtained for Figures 9 and 10 from 1-lb and 8-lb charges. This SNOW BALL film was scanned, and the transmission results have been plotted in Figure 11. Also plotted in Figure 11 are transmission data from the same 8-lb (red filter) film used in Figure 10; but the data in Figure 11 were obtained from new readings made at the time that the SNOW BALL film was scanned. (This was done to decrease uncertainties that arise in the reproducibility of readings on the densitometer.) A zero-time correction has also been made in Figure 11 to the 8-lb data from Figure 10.

The two curves in Figure 11 have not been corrected for the H&D characteristics of the Ektachrome film used; and, therefore, these curves do not represent light intensity from the explosions and should not be compared, even for relative light output. What we can correctly deduce from this figure is the time of second-shock light. From the 8-lb curve (ignoring any differences between pentolite and TNT) we find a scaled SNOW BALL time of about 250 millisecc for the second-shock-light peak. This value does not agree very well with our SNOW BALL film peak at, roughly, 285 millisecc. Further, the minimum (at about 235 millisecc) that we find in the SNOW BALL film before the second peak has not appeared on previous small-charge films. (The transmission data of the SNOW BALL curve in Figure 11 between 200 and 300 millisecc represent hundreds of frames and are thought to be physically correct.)

Comparable film transmission data have been obtained by EG&G on SNOW BALL with XR film without filters. HANSEN has reported a second-shock light maximum at 230 millisecc.

PATTMAN and TATE have reported a time of 225 millisecc from their bolometer measurements, which integrated over wavelengths from 200 to 45,000 Å and integrated over the entire surface of the fireball. Despite these differences, which we would think to be significant ones, the bolometer value agrees well with the EG&G film time.

NOLFR 67-94

Our 285-millisecond value is, thus, out of line with these two other values. We doubt that our use of the red filter could account for this difference, since the spectral differences between the bolometers and the EG&G XR film did not cause a substantial difference in these measurements. We can only guess that our field of view of the explosion, along the 296° line in the Canadian sector was different from that of EG&G in the U. S. sector. (cf. Section 3.2.1 in which radius-time data from EG&G films differ from data obtained by NOL and SES cameras in the Canadian sector.)

3.2 Pressure-Distance Curves:

Our pressure-time gages on SNOW BALL did not operate. We have derived pressure data from radius-time measurements of the luminous front produced by the explosion, as detailed in Appendices 1 and 2. Because we encountered a number of computational problems in processing the close-in SNOW BALL radius-time data, we went on to examine similar data from two shots in the SAILOR HAT series of 500-ton TNT explosions.

3.2.1 SNOW BALL: Reproductions appear in Figure 12 of color prints made from the three layers of our SNOW BALL XR* film. We could find no significant differences in the radius-time histories of the prints made through red, green, and blue filters. Because of this we made an Ektachrome copy of the original XR film for data reduction on the Telereadex film reader.**

In each frame of the film at least seven measurements of the distance to the edge of the luminous front were made, each along a different ray originating at the center of the hemisphere. The seven series of measurements were adjusted separately to $R = a_0$ (charge radius) at $t = 0$, so that zero time was set at the time light first appeared at the edge of the charge. All seven series were then lumped together and treated as a single set of data for processing (cf. Appendix 2).

Data were available from about 1.5 to 13 a_0 ($a_0 = 17$ feet) over a time interval of about 25 millisecc. The SPEC R-t curve (cf. Appendix 1 for details) is given as the solid line in Figure 13.

Several other sets of data are given in the figure for comparison:

* We are indebted to Mr. Charles Wycoff of EG&G, Inc., for making XR film available to us before it was commercially available. (For a discussion of the unique properties and use of XR film, see WYCOFF in references.)

** Our Ektachrome-through-red-filter film was not used for data reduction because no fiducial markers for size could be distinguished in the film. In our XR film the unexploded charge could be easily seen and measured.

NOLTR 67-94

- (1) The dashed curve has been taken from HANSEN for the EG&G film results.* The two curves are closely in agreement at early times (up to about 3 or 4 millisecc), thereafter the NOL curve gives larger radii at fixed times.
- (2) Pressure-gage arrival-time values, taken from Table 3.2 of REISLER - 1966, are plotted for the Ballistic Research Laboratories (BRL) data. These values appear to be slightly low but are, roughly, in agreement with the EG&G curve.
- (3) Time-of-arrival switches (ABTOADS) were used by DEWEY to obtain SES values for R-t curves. In Figure 13 we have plotted his values along the 224° line and random values along the 293° line. These SES data are rather closely in agreement with our data (taken along the 296° line and viewed perpendicular to the scene) and appear to give distinctly larger radii than those obtained by EG&G even at the latest times shown in Figure 13. This behavior suggests to us that slightly different R-t data were produced by the SNOW BALL charge along different viewing, or measurement lines.
- (4) Finally, we have plotted in Figure 13 theoretical results for a small charge scaled up to SNOW BALL conditions.** We note that for times less than about 4 milliseconds the theoretical results lie below the NOL curve, thereafter lying above the EG&G curve and below the NOL curve.

* A value of 0.76 msec has been subtracted from EG&G times to reduce them to our $t = 0$ at $R = 17$ ft measurements. This value is based on a nominal detonation speed of 6800 m/sec. Probe measurements on SNOW BALL gave a value of 6720 ± 50 m/sec (from a letter of 2 November 1964 by W. J. Ditto of SES).

** We are indebted to D. L. Lehto for making this special computer run (WUNDY 1327) for us. The computation was made for a 1-lb TNT sphere at sea-level conditions with millimeter-zone resolution. (Results of similar computations have been reported by Lutzky, M., "Theoretical Versus Experimental Results for Air Blast from One Pound Spherical TNT and Pentolite Charges at Sea Level Conditions," NOLTR 65-57, 1 July 1965.) These WUNDY results were then scaled up to 1000 tons of TNT at $p_0 = 13.60$ psi for presentation in Figure 13. Temperature scaling was thought to be insignificant and was omitted.

In Figure 14 we have plotted velocity-distance curves which have been processed from film measurements by NOL, EG&G, and SES. We note that these curves are rather different in curvature until about $R = 150$ ft. Pressures that would be computed from such curves would be even more different, since pressure is proportional to the square of velocity - through the Rankine-Hugoniot relations.

3.2.2 SAILOR HAT: The charges used in the SAILOR HAT series were similar to the SNOW BALL charge - nominal 500-ton weight, block construction, and large-grain TNT castings. We doubt that we could have detected any differences in the films that could have arisen from differences that existed in the type of TNT, in the detonation details or in the nature of the ground beneath the charges.

Several SAILOR HAT films were made available to us* and from these we selected one from Event B (EG&G film No. 98107), and one from Event D (EG&G film No. 98307) each of which contain R-t data in a range comparable to SNOW BALL.

Both Event B and D films were read in the same way the SNOW BALL film was: 7 ray-radii were determined in each frame; each was adjusted so that $R = a_0$ at $t = 0$, and all rays were lumped for fitting by SPEC. Both these films contained data far beyond the range of the SNOW BALL data; but only the data over the range roughly to $14 a_0$ were used to make comparisons.

Figure 15 compares the SPEC fits to the SAILOR HAT and SNOW BALL data. The Event B curve is about 10 per cent below the SNOW BALL curve; for all practical purposes, the Event D curve coincides with the SNOW BALL curve. Comparisons of the fitted SPEC curves with the original film data indicate that the average deviations in fitted distance at a given time were:

SNOW BALL	2.12 per cent
SAILOR HAT B	2.49
SAILOR HAT D	2.15.

If we assume that all the 500-ton charges behaved identically in the three explosions of Figure 15, then we can, further, assume that the spread between the curves of Figure 15 is a measure of the uncertainty to be expected in reading and fitting the radius-time data of an arbitrary explosion of similar characteristics.

* We are indebted to Mr. D. F. Hansen of EG&G, Inc., for making copies of these films available to us. Both films were made by a Photo-Sonic 4c camera on XR film. Frame rate of No. 98107 was 2456 fps; No. 98307, 2380 fps.

3.2.3 Pressure-Distance Comparisons: In Figure 16 we have drawn the pressure-distance curves computed from the SPeC fits for three 500-ton shots. If we, again, assume that all three explosions behaved identically, then the spread between these curves gives a measure of the uncertainty that must be tied to such computed pressure curves. We note that the SAILOR HAT curves are almost identical but slightly displaced and that the SNOW BALL curve lies bounded by these SAILOR HAT extremes.

Also plotted in Figure 16 are BRL pressure-gage readings taken from REISLER - 1966 for SNOW BALL and from REISLER - 1967 for SAILOR HAT. These measurements are about a factor of 2 lower than our computed pressures in the pressure range above about 400-500 psi. Below this pressure level the two sets of measurements appear to be coming together.

Few measurements of shock pressures in the range hundreds to thousands of psi have ever been made. There are many difficulties both in the use of gages and in the use of film data and we cannot be sure which set of data in Figure 16 is correct, if either is.

To examine the situation, we have plotted several sets of data in Figure 17.*

- (1) Our SNOW BALL curve of Figure 16 is replotted here as the solid curve; the solid symbols for the BRL gage data are also simply redrawn from Figure 16.
- (2) The dashed curve has been taken from KINGERY and PANNILL and represents results from 5-, 20-, and 100-ton TNT hemisphere explosions that preceded the SNOW BALL shot. Included in the compilation were both gage measurements and film measurements.
- (3) Plotted as crosses are theoretical results (WUNDY 1327) from a calculation of a 1-lb sphere of TNT (at sea level) and scaled up to SNOW BALL conditions by assuming the yield to be 1000 tons and taking the ambient pressure $p_0 = 13.60$ psi. We note that the NOL curve and the WUNDY results agree reasonably well until about 3000

* We have omitted the pressure-distance curve for SNOW BALL given by DEWEY for the SES measurements. This curve, obtained shortly after the explosion, was not corrected for real-gas effects which are extremely important in the pressure range examined in Figure 17.

NOLTR 67-94

psi when the theoretical pressures drop below the NOL curve. The WUNDY values lie between the NOL curve and the BRL curve, appearing to converge into the 500-ton gage pressures at about the 100-psi level

- (4) Plotted as open circles are the pressures computed from our SPEC fit to the EG&G results for SNOW BALL. The input radius-time data used to obtain these pressures were taken from the EG&G curve shown in Figure 13.

We can make no firm conclusions from Figure 17. BRL gage pressures do appear to be significantly lower (until 400-500 psi) for the three 500-ton explosions than previous pressures from 5-, 20-, and 100-ton explosions.

In the early stages of the 500-ton explosion, we could expect explosion behavior rather much like a one-dimensional 500-ton spherical explosion. In Figure 17, we note that the WUNDY one-dimensional results (for 1000 tons) are slightly higher than the NOL curve for SNOW BALL at close-in distances. Two-dimensional effects, because of the use of block charges and of effects from the reflecting ground surface beneath the SNOW BALL charge, could overwhelm the one-dimensional explosion growth at slightly later times. We would not expect these two-dimensional effects to be very large; but such effects could lead to a factor greater than 2, which value would be obtained in going from a hemisphere to a sphere in purely one-dimensional symmetry. Examining Figure 17, we do note that the theoretical results lie below the NOL curve after about the 3000-psi level, as we might expect. But the NOL curve seems to bulge away from the WUNDY results excessively from about 3000 to 1000 psi. We suspect therefore that the NOL curve is too high and should be lowered about 10 to 20 per cent in this region. Even if this were to be done, however, the pressure-gage data would still be considerably lower than our pressures derived from film data.

The EG&G pressures appear to agree better with our theoretical WUNDY pressures and are consistently lower than our NOL curve. Since both sets of experimental data (NOL and EG&G) were processed by the same computer program, the differences between the NOL curve and the EG&G pressures must be ascribed to experimental differences. Such differences could have been produced in reading of the camera films. But the distinctly different behavior, at times, later than, say, 2 millisecc, of the NOL and the EG&G radius time curves of Figure 13 suggests to us that the growth of the SNOW BALL explosion seen by the EG&G cameras was different from the growth that we viewed.

NOLTR 67-94

Whatever the explanation for the differences in the pressures derived from the NOL and EG&G films, we note that these differences are small compared to the differences between these derived pressures and the pressure-gage values at levels above, say, 1000 psi. In the region, hundreds of psi, the scatter in the pressure-gage values of Figure 17 appears to be comparable to the differences between the "average" film value and the "average" gage value.

4. DISCUSSION

From a number of integrated measurements that we had planned for SNOW BALL, we obtained only three records. Because of this we are not able to reach any significant conclusions from these records alone. But by making comparisons of these records with results obtained on other explosions, we have been able to make certain observations on the SNOW BALL-explosion behavior, which have been discussed in Section 3.

Here, we summarize and assess the significance of the more important of these observations:

4.1 Radiation Measurements:

- a. The identifiable features of the SNOW BALL spectrum come from a number of impurity radiators, such as sodium, calcium, and cyanogen, plus forbidden bands of oxygen (Herzberg and night-sky). We have not detected any radiators that we might expect from shocked air (at equilibrium), such as N_2 or NO bands. We have not seen any evidence of NO_2 absorption which might be expected to occur ahead of a strong airshock. The existence of continuum radiation is not clear; but we doubt that such radiation occurred on our SNOW BALL spectrum.
- b. Certain radiant features may cube-root scale with charge weight⁺ others do not. The earliest portion of the SNOW BALL thermal pulse (light intensity vs. time) appears to cube-root scale the pulse from a 100-lb TNT sphere. But similar records from 8- and 32-lb TNT spheres do not scale. The time for second-shock brightening may cube-root scale from small charges to 500 tons.
- c. Photographic data, such as radius-time data and time of second-shock brightening, from SNOW BALL appear to vary with the field of view of the explosion. Spectral details may vary substantially from charge to charge and may depend upon the precise chemical and physical characteristics of the charge.

4.2 Pressure Measurements:

- a. Pressures, derived from film radius-time data, for SNOW BALL and two SAILOR HAT explosions (all 500-ton TNT hemispheres) are in

reasonable agreement with each other (few per cent) and with scaled-up theoretical pressures for a 1-lb sphere.

- b. These derived pressures, however, are about a factor of 2 higher than the pressure-gage measurements on 500-ton explosions. Further, these measurements are also significantly lower than would be expected from previous pressure-gage results on 5-, 20-, and 100-ton TNT hemisphere explosions. These differences exist above the 400-500 psi level; below this pressure level all values begin to approach one another.

The significance of these observations lies in the following discussion:

The early light produced by a chemical explosion has been often, if not universally, considered to come from a luminous airshock that advances ahead of the explosion gases. Because of this, measurements of the position of the advancing luminous front would be taken to be also measurements of the air shock, since they are one and the same front. Airshock pressures, therefore, are derivable from these luminous-front measurements by use of the usual hydrodynamic conservation equations.

Our spectral data, however, for SNOW BALL (and for small charges) do not indicate to us the existence of shocked air. We base this both on spectral species and on failures in cube-root scaling, which we believe should hold if luminosity is intimately tied to hydrodynamics. Such shocked-air radiation may, indeed, exist and have been below the level of detectability of our instrumentation. The key point, however, is that the preponderant portion of explosion light is not directly produced by shockfront reactions in air.

There may well be direct dependence of the explosion light on the airshock details but that dependence remains to be found. We no longer can be confident that the early luminous-front motion is identically the airshock motion.* And, because of this, we can no longer be confident that hydrodynamic pressures derived from luminous-front motion have meaning.

* Our unreported small-charge results suggest that a nonluminous airshock travels at the front of the luminous radiation and begins to separate at a few charge radii.

Our derived pressures from SNOW BALL and SAILOR HAT luminous-front motion are considerably higher than the pressure-gage values - a factor of 2 - in the high-pressure region (roughly 5000 to 400 psi). If the luminous-front motion and the airshock motion were not well coupled on these 500-ton explosions, we might expect to find large differences between real hydrodynamic pressures which gages read and pressures derived from luminous-front motion. If this were the case, we have no problem: the gages have measured real pressures and our derived pressures would simply be meaningless.

But the situation is not so simple. Firstly, if we compare the measured 500-ton hemisphere pressures with earlier 5-, 20-, and 100-ton hemisphere pressures we find that the 500-ton values are distinctly lower (Fig. 17) than we expect from scaling-up the earlier pressures. Secondly, if we compare our derived pressures with theoretical predictions for an ideal, classical one-dimensionally spherical explosion, we find that there are differences but that these are not large - not large compared to a factor of 2 at any event. Further, the disagreements seem small enough to suggest that the motion of the luminous-front and of the airshock are coupled rather well.

We therefore reach the following dilemma:

- a. The 500-ton gage pressures are wrong (in the pressure region above 400-500 psi), for reasons unknown;
- b. the derived pressures are wrong, either for computational reasons or because the airshock and luminous front are not well coupled;
- c. both sets of results are right (or wrong) but are measuring different phenomena.

We have not clearly covered all possibilities in the three above; for example, our cameras on SNOW BALL did not look at the explosion along the line of the pressure gages. Perhaps the charge itself produced irregular, unsymmetric phenomena. Some evidence exists to support this in the different radius-time data found from NOL, SES, and EG&G films on SNOW BALL.

We are well aware of many uncertainties in the various steps that must be followed to derive pressures from films; and we have tried to limit these uncertainties as much as possible. We have described in this report only the final procedure that we used to process the film data for pressures. We have not discussed many other procedures that we investigated and discarded. Our diligence

HOLTR 67-94

does not, of course, guarantee the accuracy of our derived pressures. But the comparisons of these pressures with related pressures, as in Figures 16 and 17, does give us some confidence that our derived pressures look reasonable.

We are not so aware of the uncertainties in using pressure gages in the 5000-200 psi region; but we do not doubt that a number of uncertainties must exist close-in to an explosion, where ionization and electromagnetic fields are at their largest values.

At the present time we see no satisfactory explanation for the factor-of-2 difference between gage- and derived-pressures and we suggest that explorations be made in future investigations.

5. REFERENCES

ALLEN, Richard A., "Air Radiation Tables," NASA Contractor Report CR-557, August 1966; "Air Radiation Graphs," NASA Contractor Report CR-556, August 1966

DEWEY, John M., "Measurement of Free Field Overpressure," in G. H. S. Jones: "Preliminary Report on the Canadian Projects in the (1964) 500-Ton TNT Suffield Explosion," Suffield Special Publication 45, December 1964

ERICSSON, U., "Om Lysande Luftstoetvaagor (On Luminous Air Shock Waves) Part III," Defense Research Institute, Stockholm, 12 September 1956

HANSEN, D. F., JOHNSON, A. C., and HALL, W. N., "Technical and Fireball Photography on Operation SNOW BALL," DASA-1593, EG&G B-2936, 10 May 1965, Confidential

KINGERY, C. N. and PANNILL, B. F., "Peak Overpressure Versus Scaled Distance for TNT Surface Bursts (Hemispherical Charges)," BRL Memorandum Report No. 1518, April 1964

PATMAN, J. D. R. and TATE, P. A., "Surface Burst of 500-Ton TNT Hemispherical Charge (1964); Project No. 4 Thermal Measurements," DCBRL Report No. 488, May 1966

HEISLER, R. E., KEEFER, J. H. and GIGLIO-TOS, L., "Basic Air Blast Measurements from a 500-Ton TNT Detonation, Project 1.1 Operation SNOW BALL," BRL Memorandum Report 1818, December 1966

HEISLER, R. E., RALEY, R. J., and LE FEVRE, D. P., "Air Blast Measurements Recorded by Standard and Developmental Instrumentation - Operation SAILOR HAT; Project Officers Report, Projects 1.1, 1.4," BRL Draft of 28 March 1967

HUDLIN, L., "On the Origin of Shockwaves from Condensed Explosions in Air, Part 1: Results of Photographic Observations of Pentolite Hemispheres at Ambient Conditions," NOLTR 62-182, 9 November 1962

HUDLIN, L., "On the Origin of Shockwaves from Condensed Explosions in Air, Part 2: Measurements of Airshock Pressures from 8-lb TNT Spheres of Various Densities at Ambient Pressures," NOLTR 63-13, 21 January 1963

WYCOFF, Charles W., "An Experimental Extended Exposure Response Film," S.P.I.E. Newsletter of June-July 1962

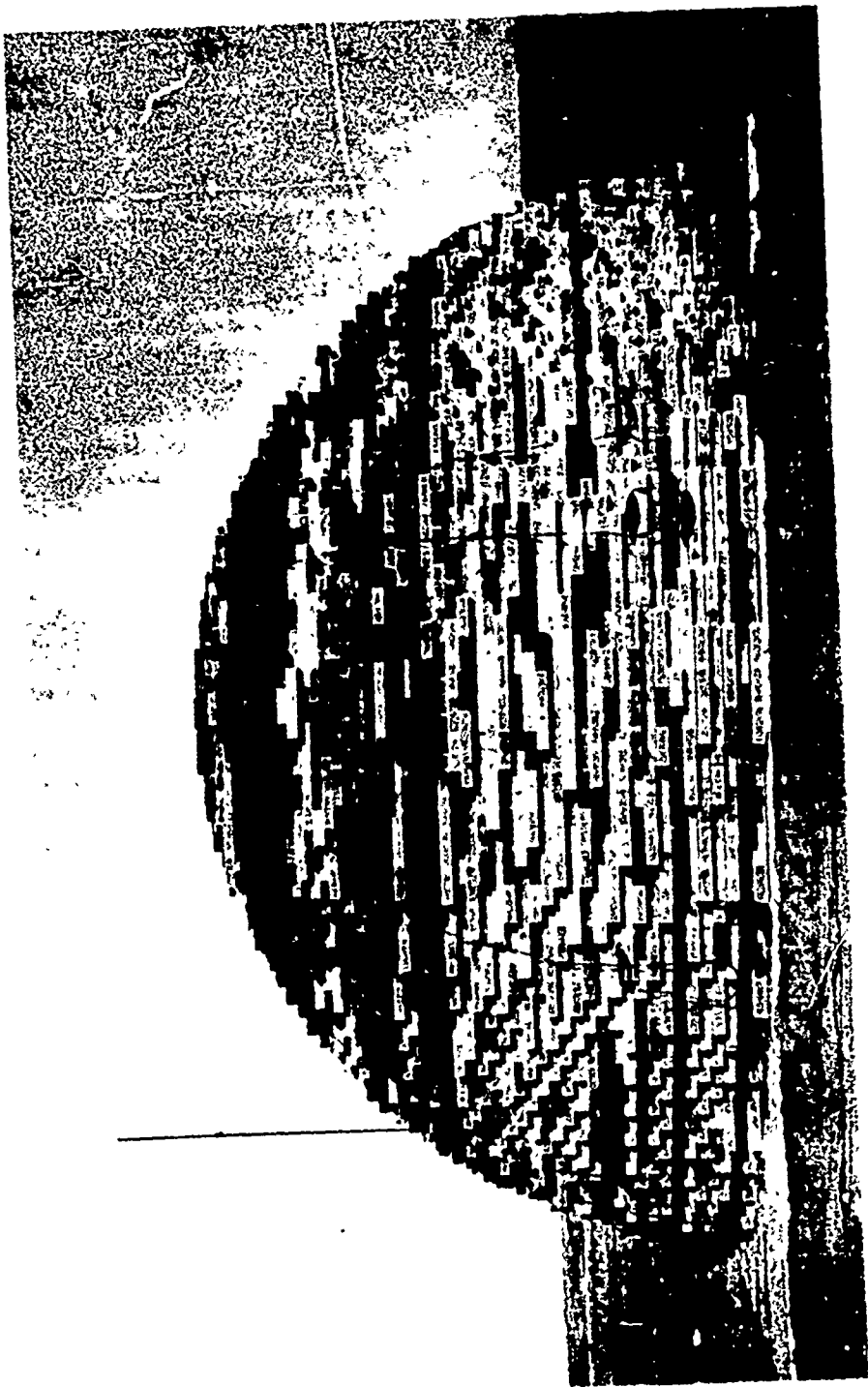


FIG.1 SNOW BALL CHARGE IN POSITION FOR FIRING - CHARGE RADIUS ~ 17 FEET

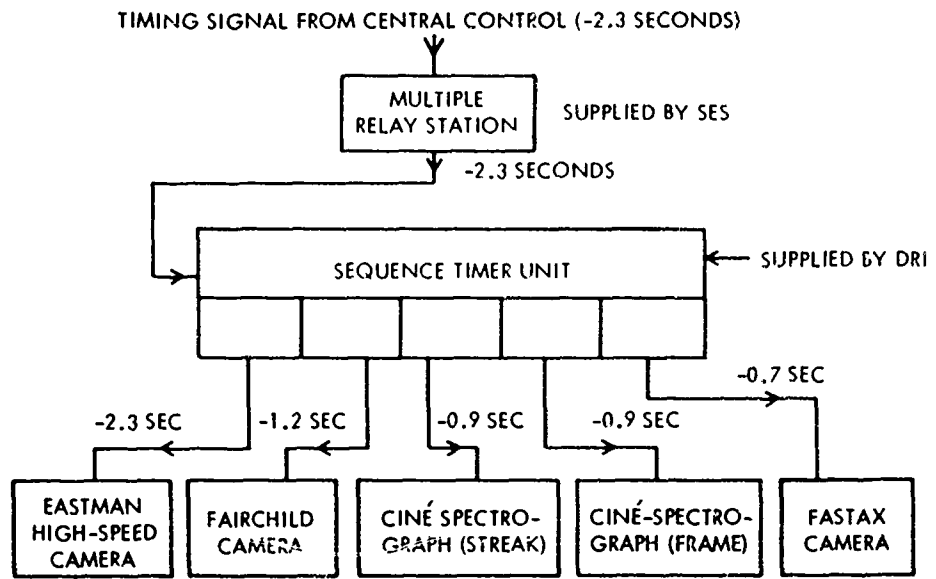


FIG.2a BLOCK DIAGRAM OF TIMING SEQUENCE FOR HIGH SPEED CAMERAS AND CINÉ-SPECTROGRAPHS

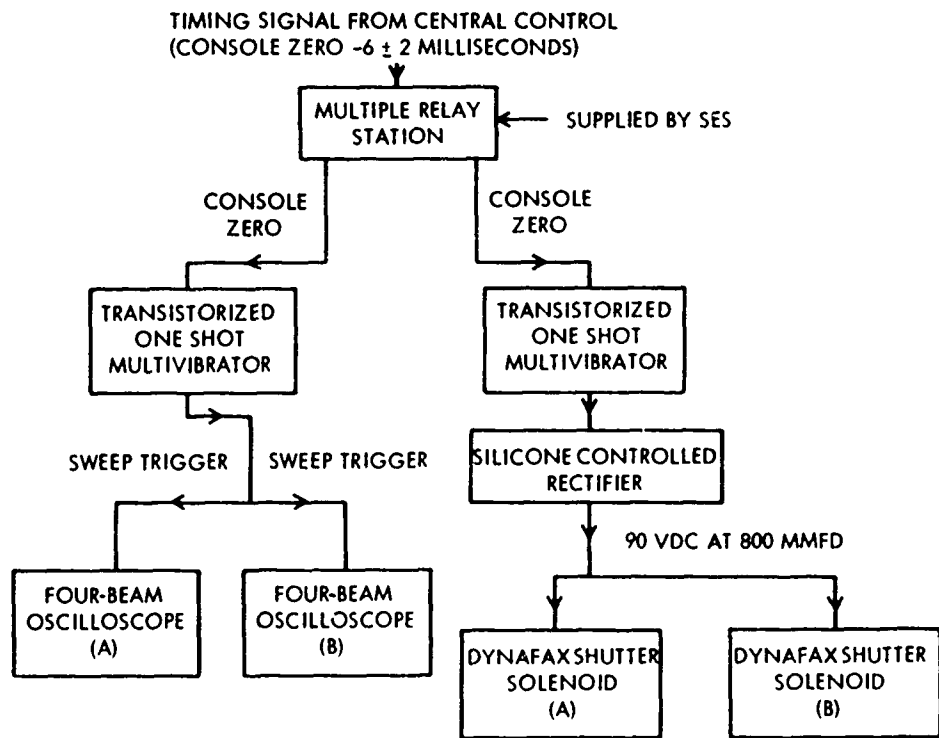


FIG.2b BLOCK DIAGRAMS OF TIMING SEQUENCE FOR FOUR-BEAM OSCILLOSCOPES AND DYNAFAX CAMERAS

NOLTR 67-94

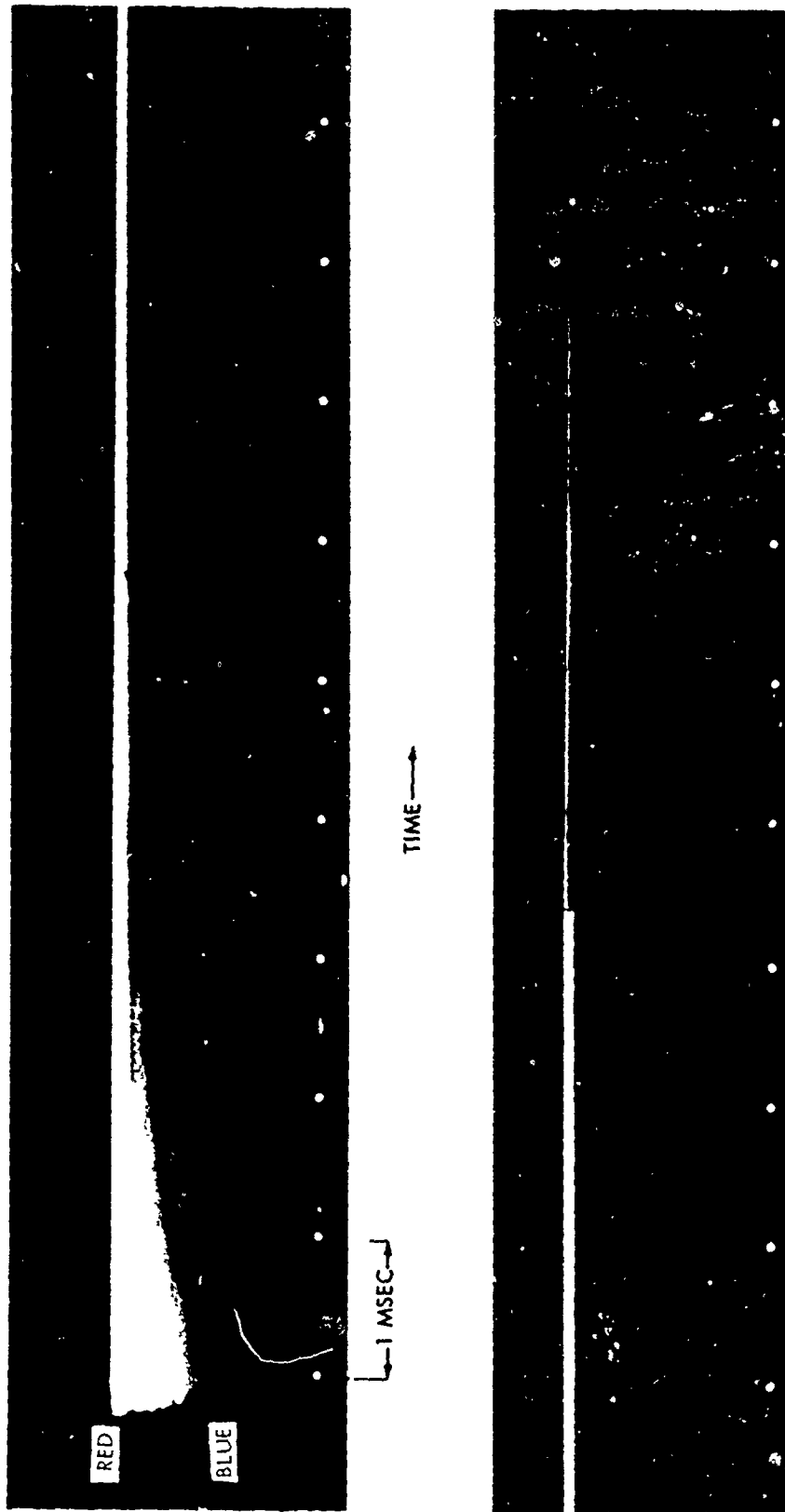


FIG.3 STREAK SPECTRUM OF SNOW BALL

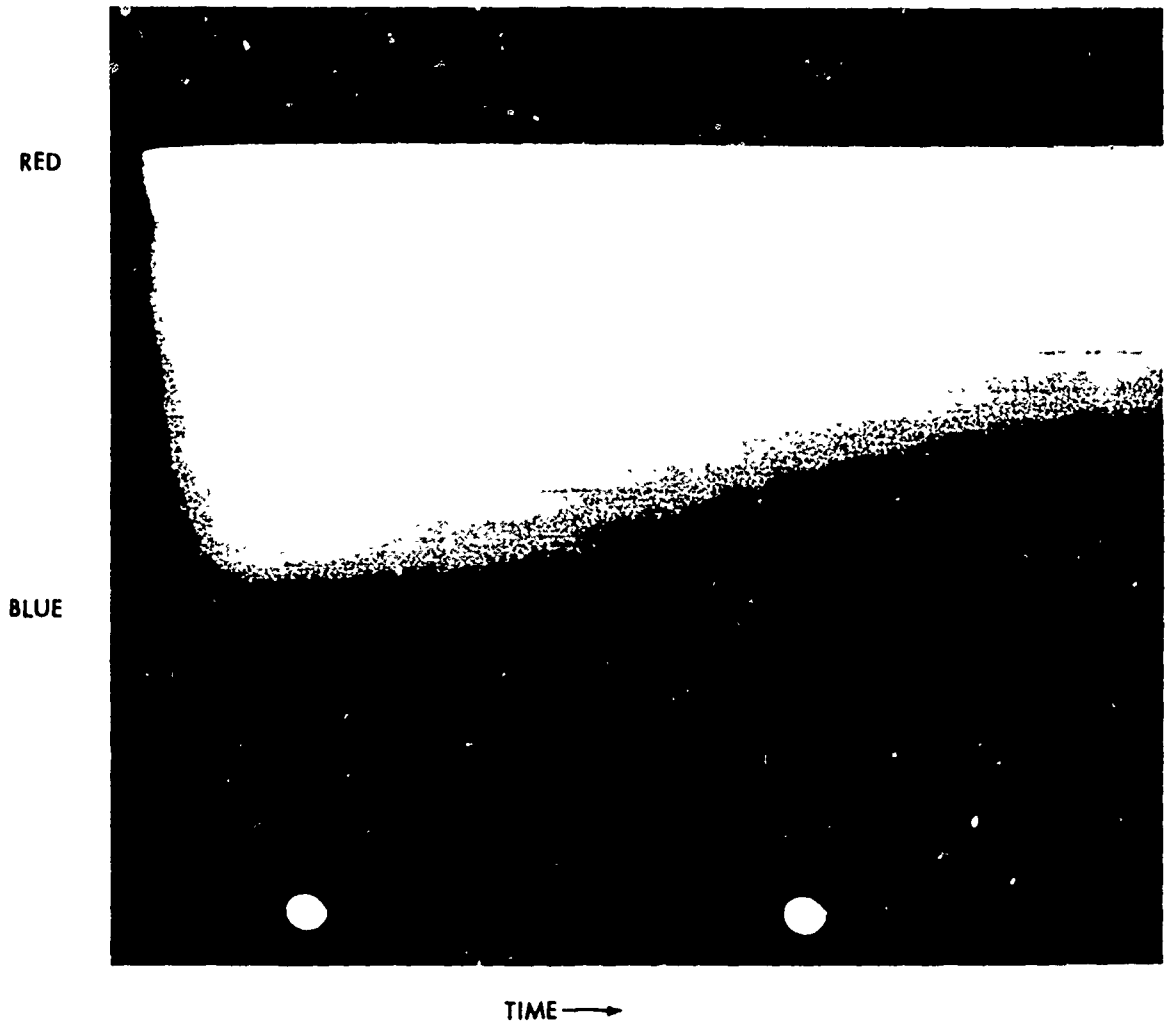


FIG.4 ENLARGEMENT OF THE FIRST MILLISECOND OF SNOW BALL SPECTRUM

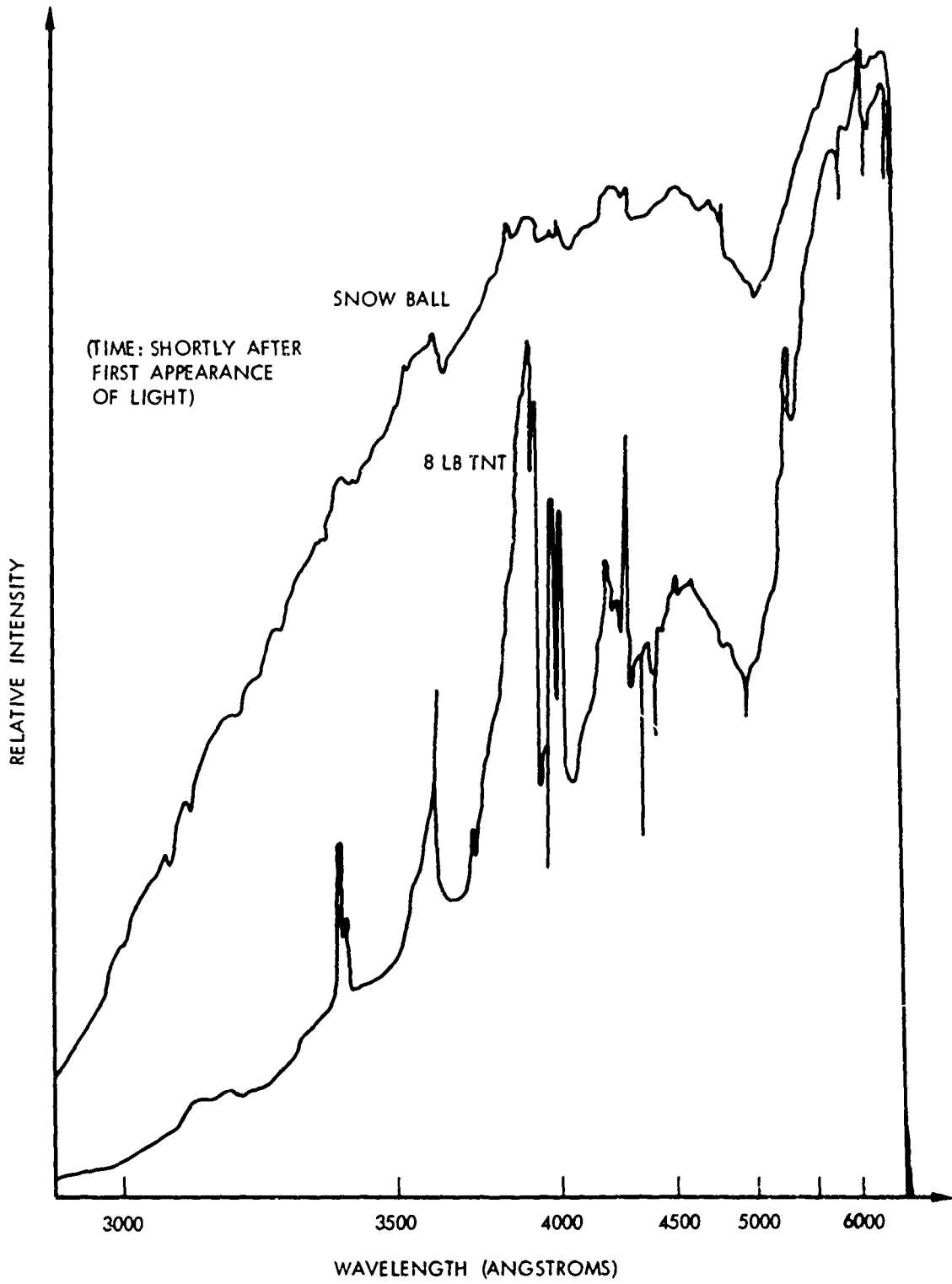


FIG. 5 COMPARISON OF DENSITOMETER TRACINGS OF STREAK SPECTRUM FROM SNOW BALL AND FROM TYPICAL 8-LB TNT SPHERE

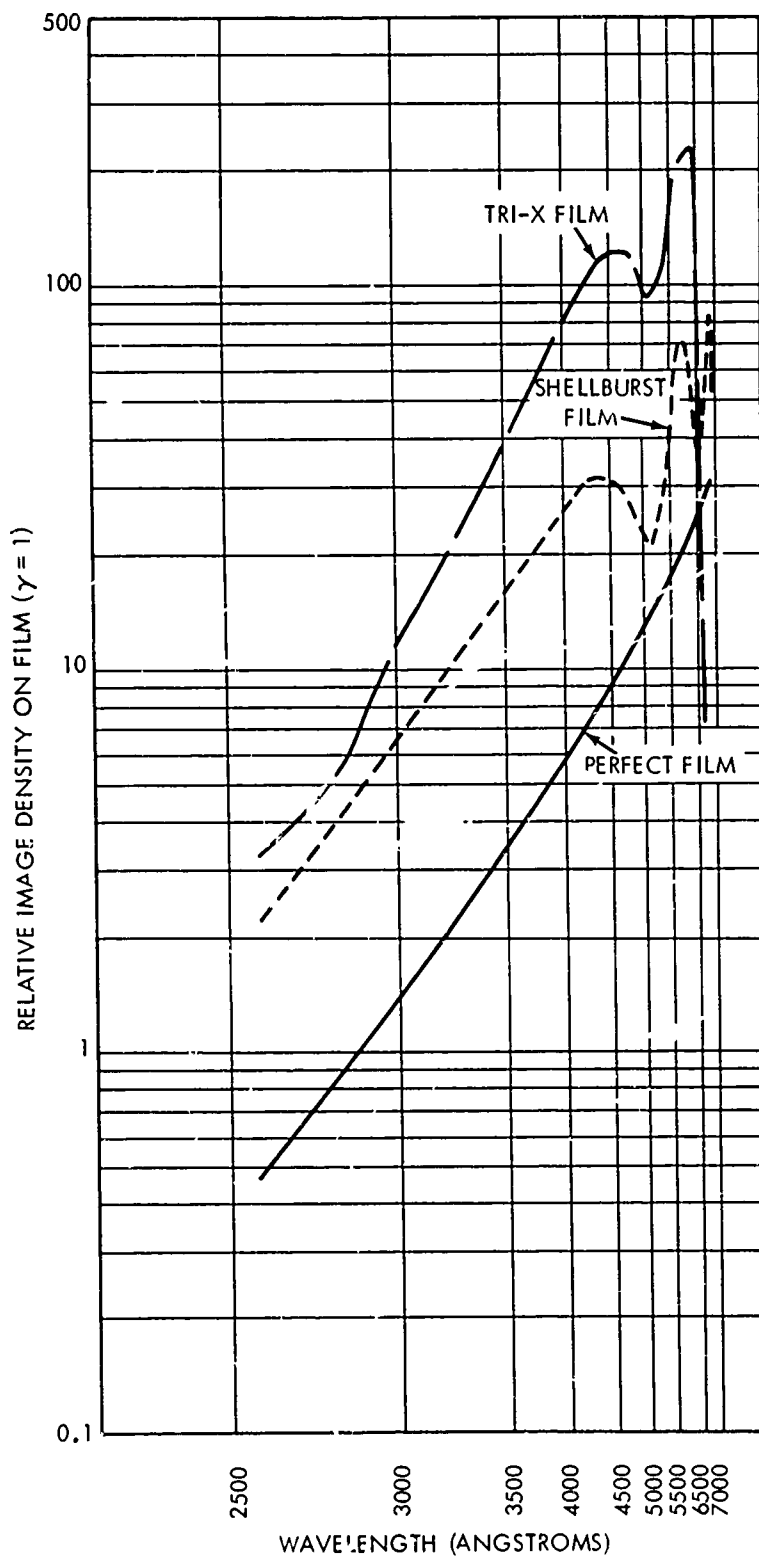


FIG. 6 STREAK CINE-SPECTROGRAPH IMAGE DENSITY RESULTING FROM VIEWING 6000°K BLACKBODY SOURCE



C. 100 LB SPHERE



B. 32LB SPHERE



A. 8 LB SPHERE

FIG.7 COMPARISON OF MILLISECOND SPECTRA FROM SMALL TNT SPHERES

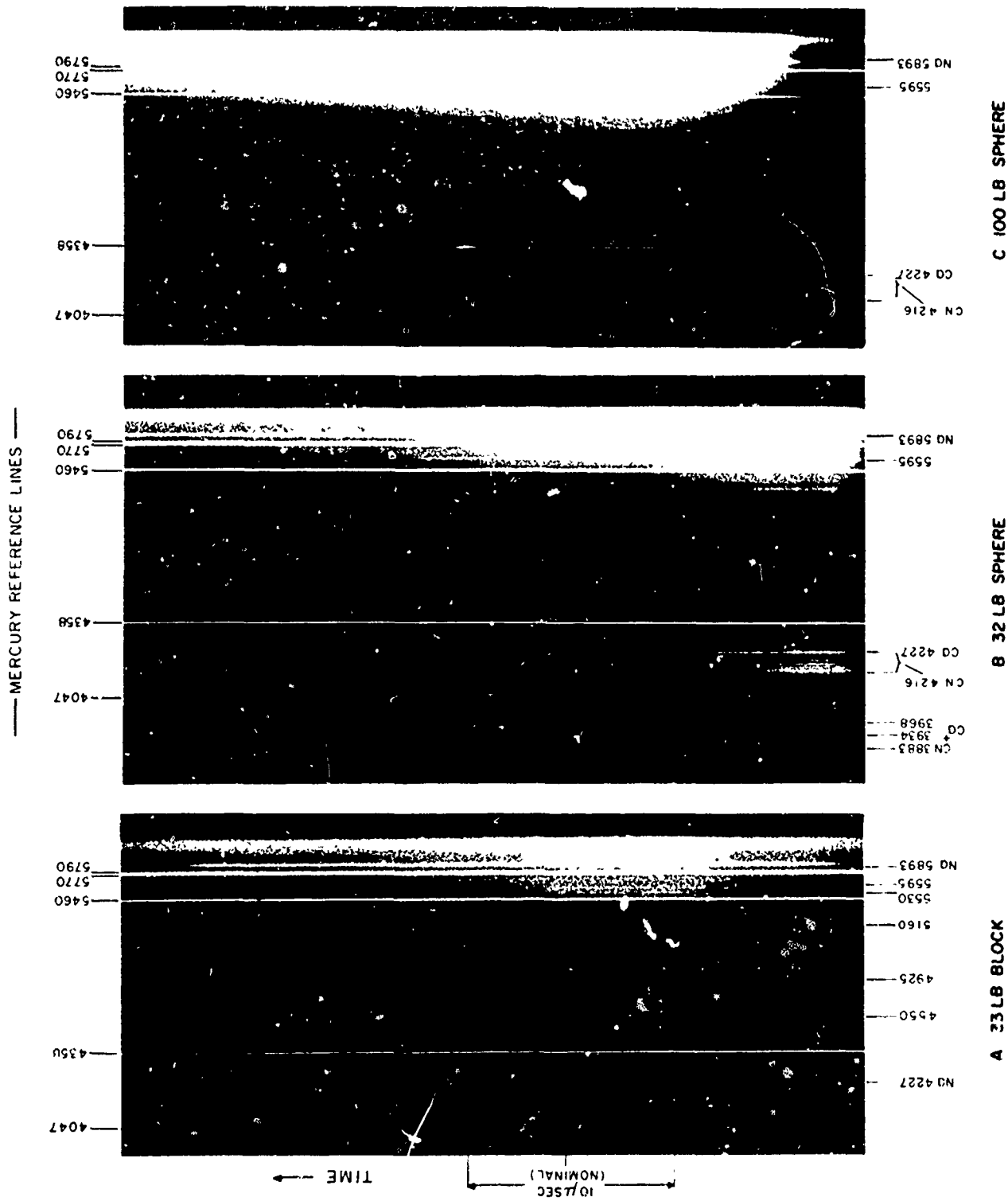


FIG. 8 COMPARISON OF μ SEC SPECTRA FROM VARIOUS TNT CHARGES

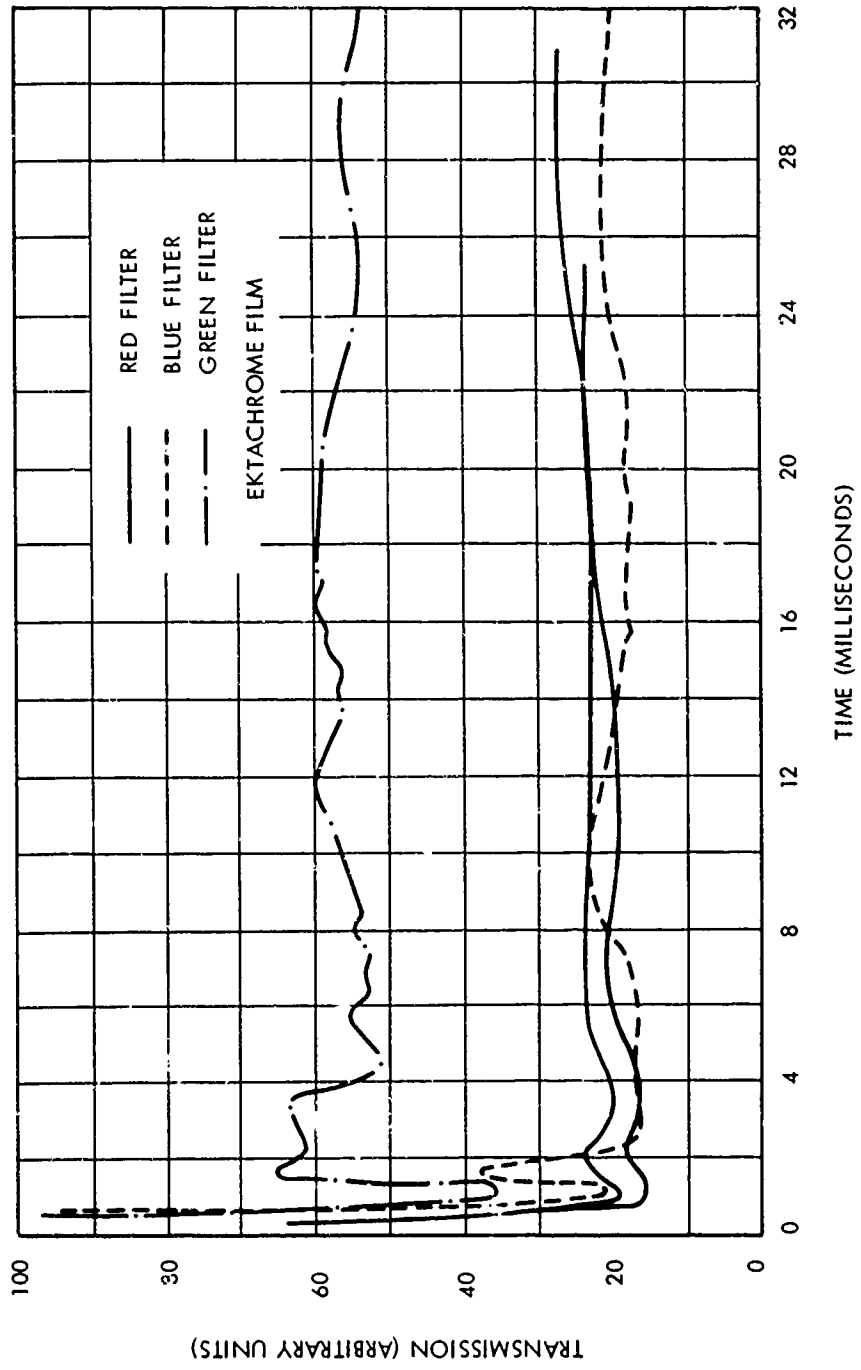


FIG. 9 EXPLOSION LIGHT VS TIME (1-LB PENTOLITE SPHERES)

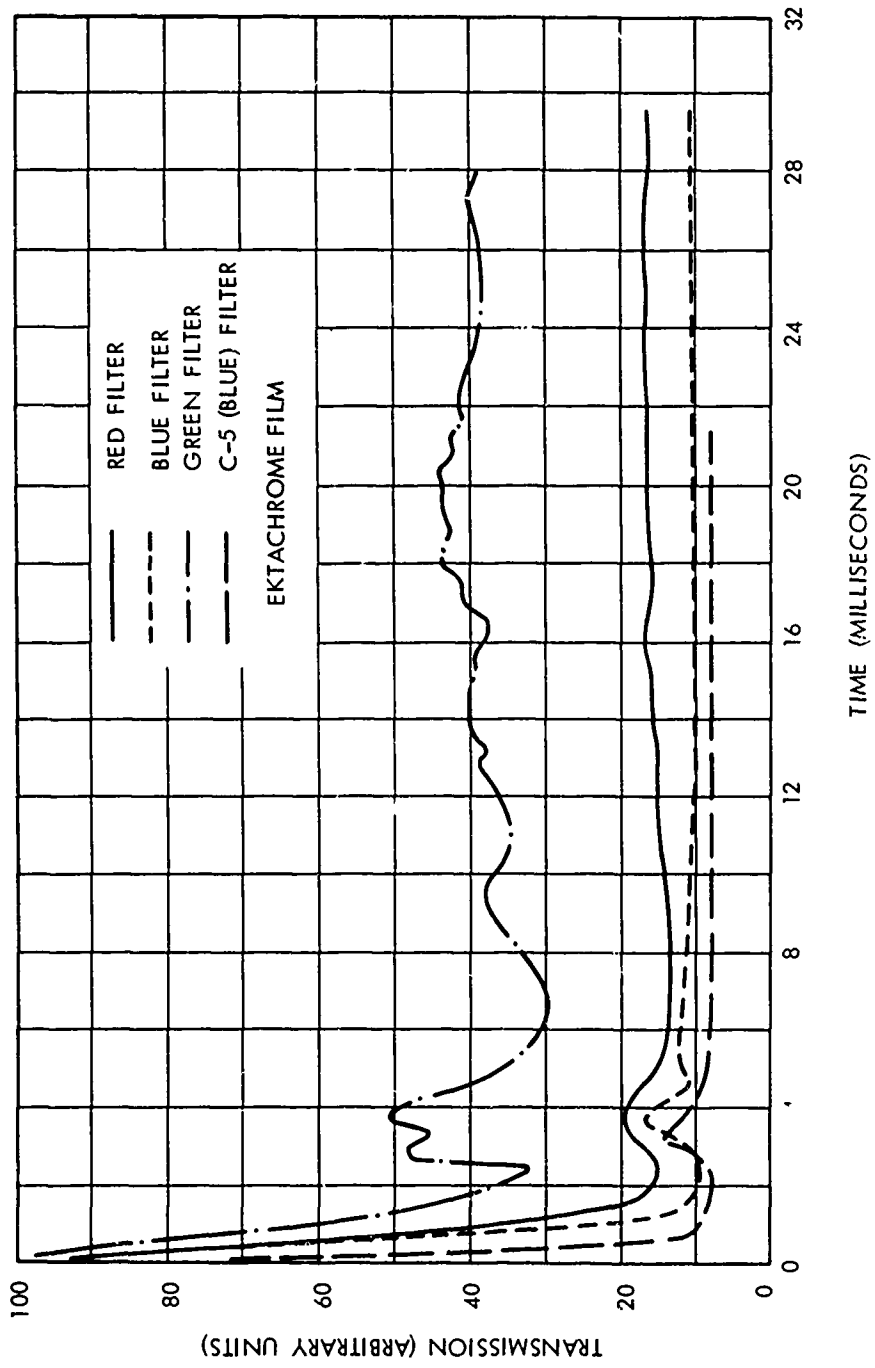


FIG. 10 EXPLOSION LIGHT VS TIME (8-LB PENTOLITE SPHERES)

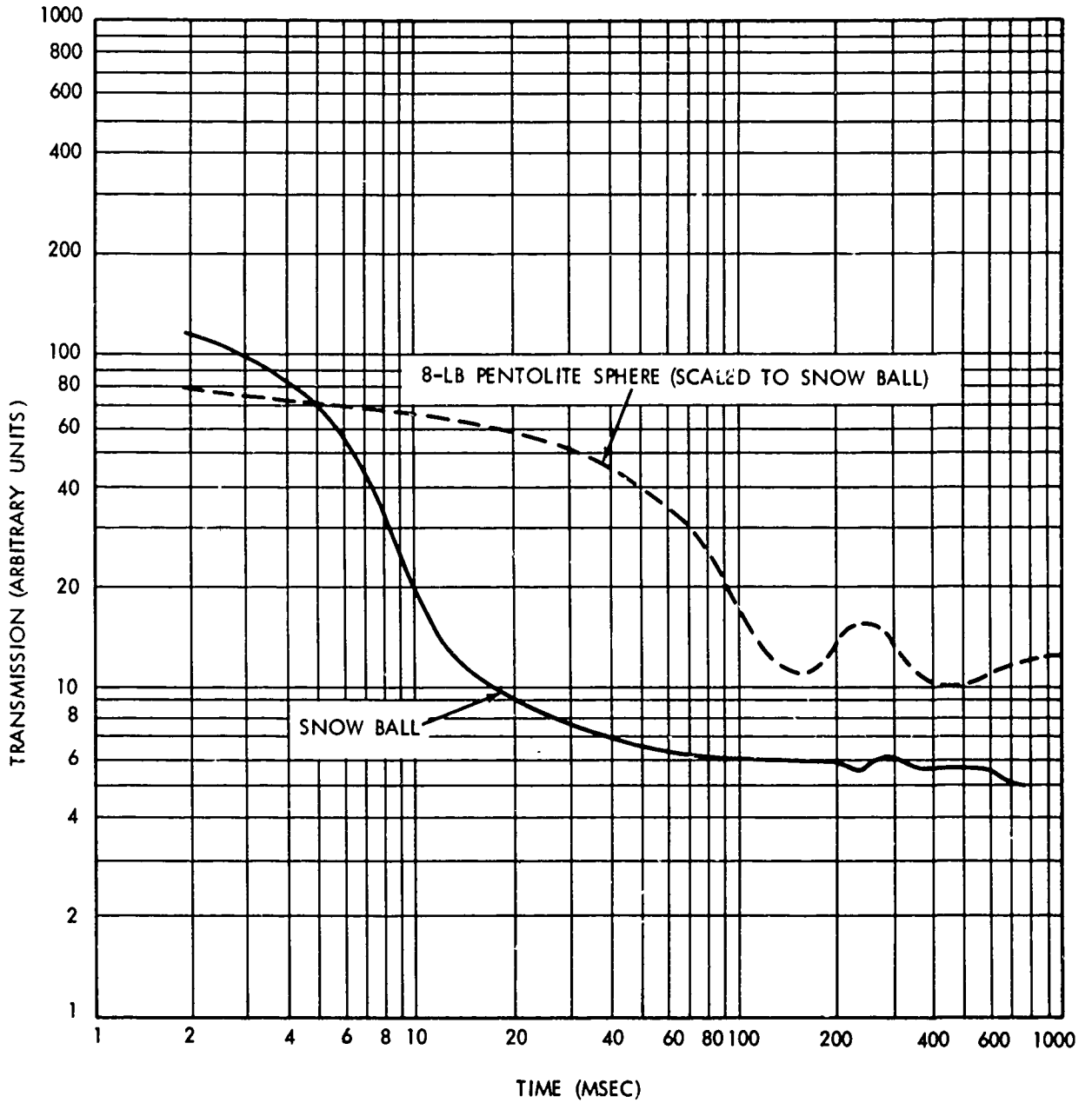
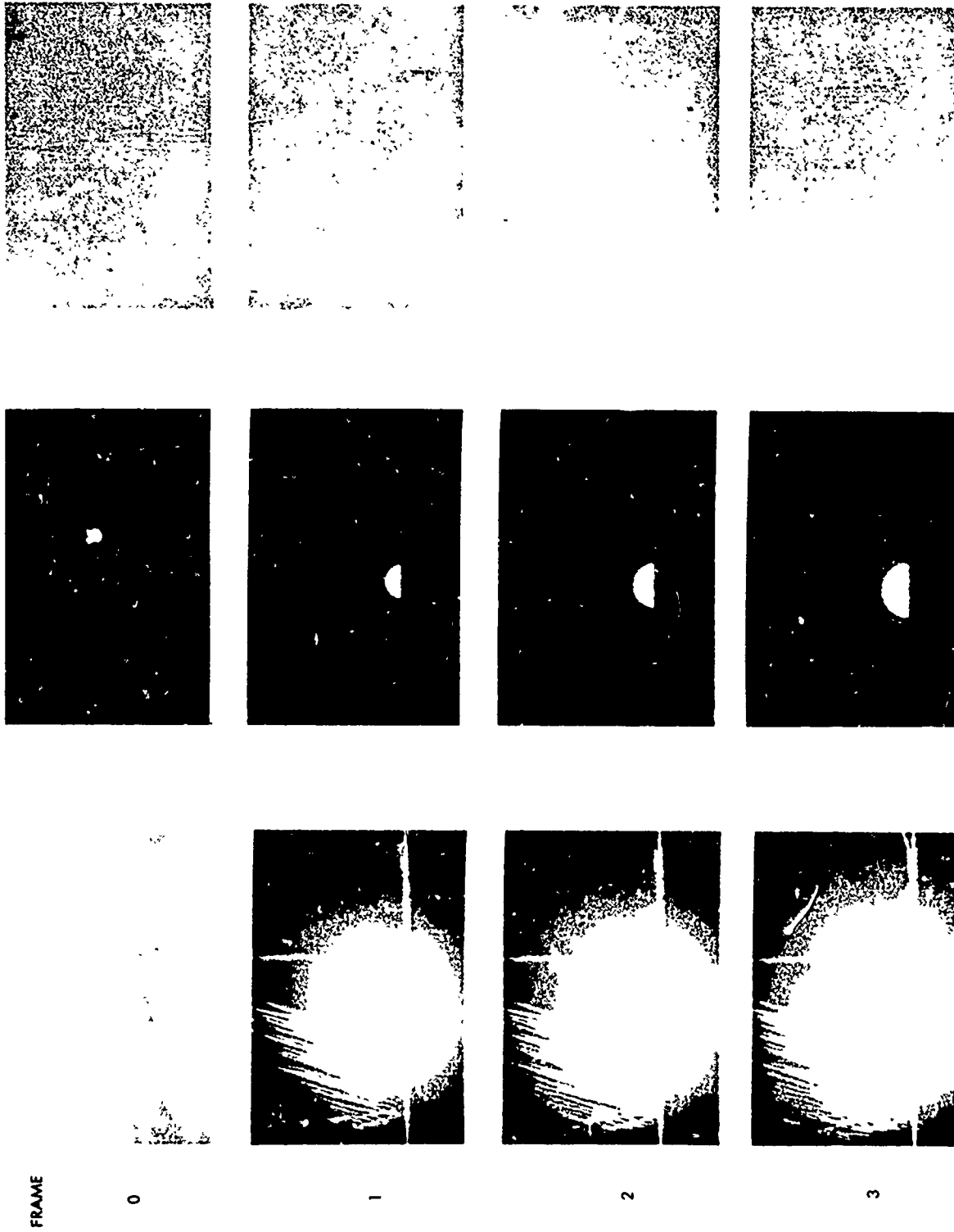


FIG. 11 COMPARISON OF EXPLOSION LIGHT FROM SNOW BALL AND FROM A SMALL CHARGE



RED FILTER

BLUE FILTER

GREEN FILTER

FIG. 12a SNOW BALL MOTION AT 2611 FPS ON XR FILM

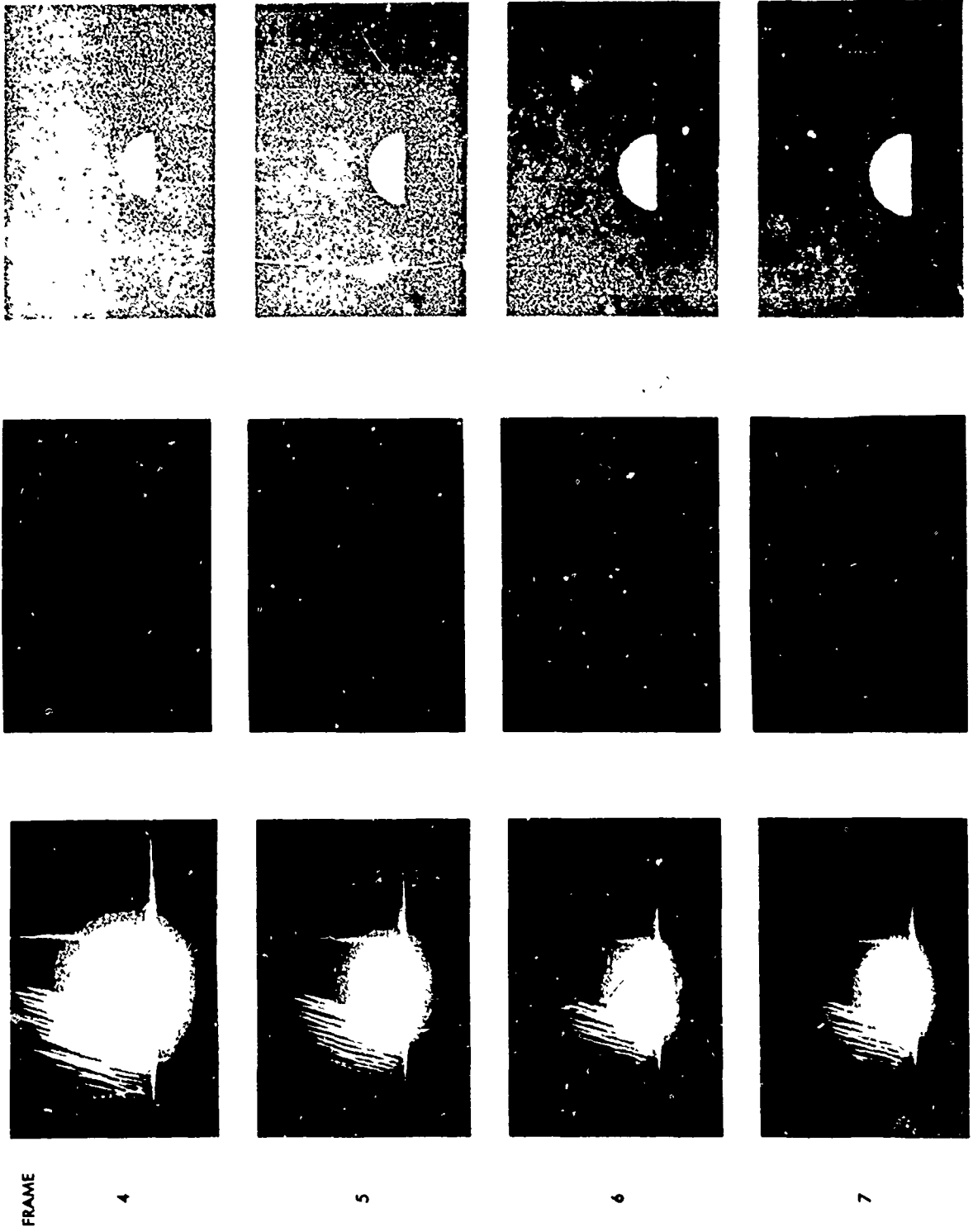
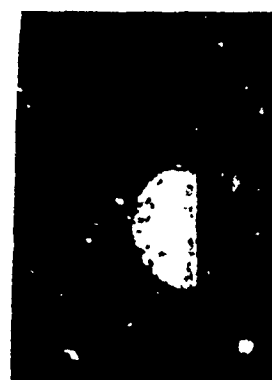
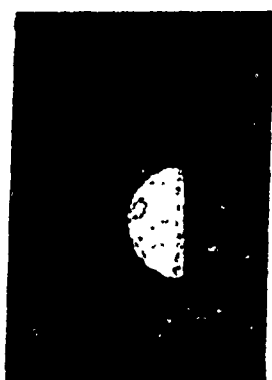
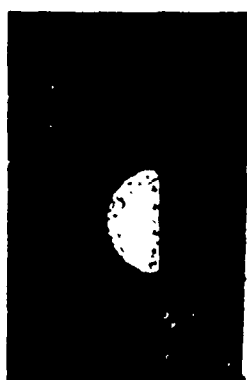
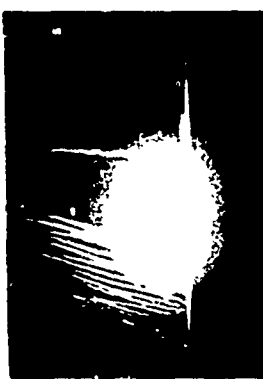


FIG. 12b SNOW BALL MOTION AT 2611 FPS ON XR FILM



RED FILTER



GREEN FILTER

FRAME

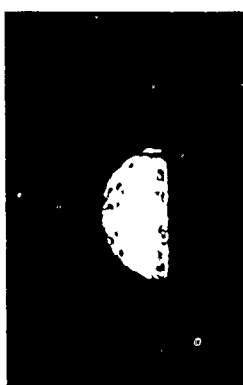
8

9

10

11

FIG. 12c SNOW BALL MOTION AT 2611 FPS ON XR FILM

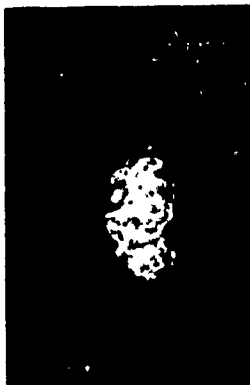


FRAME

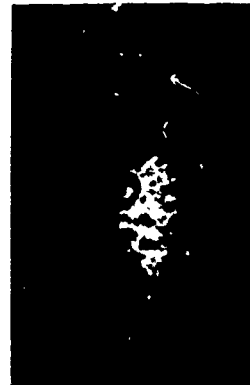
12



13



14

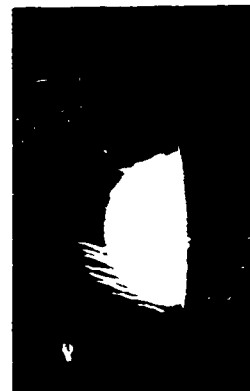


15

GREEN FILTER



BLUE FILTER



RED FILTER

FIG. 12d SNOW BALL MOTION AT 2611 FPS ON XR FILM

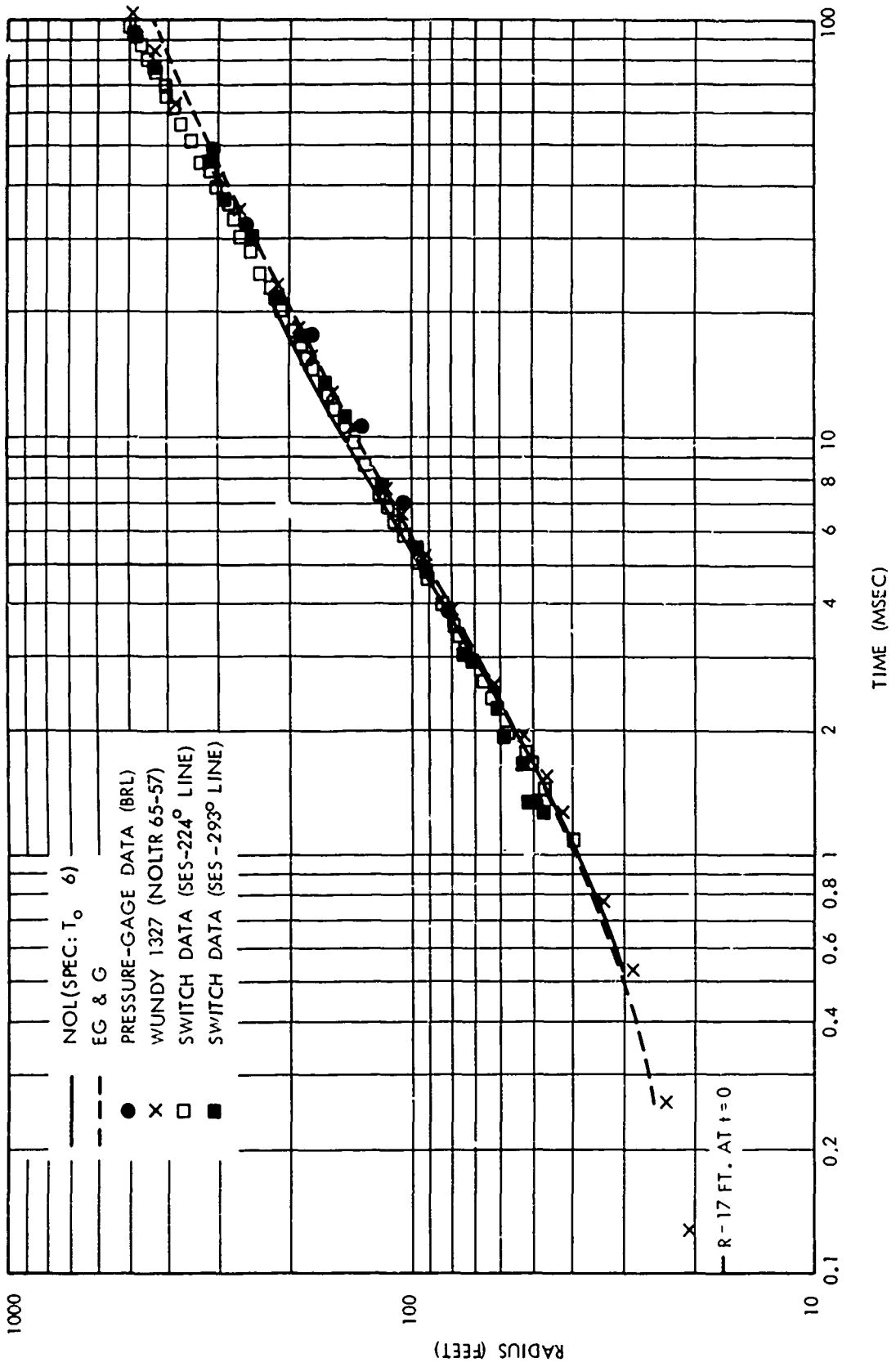


FIG. 13 SNOW BALL RADIUS-TIME GROWTH

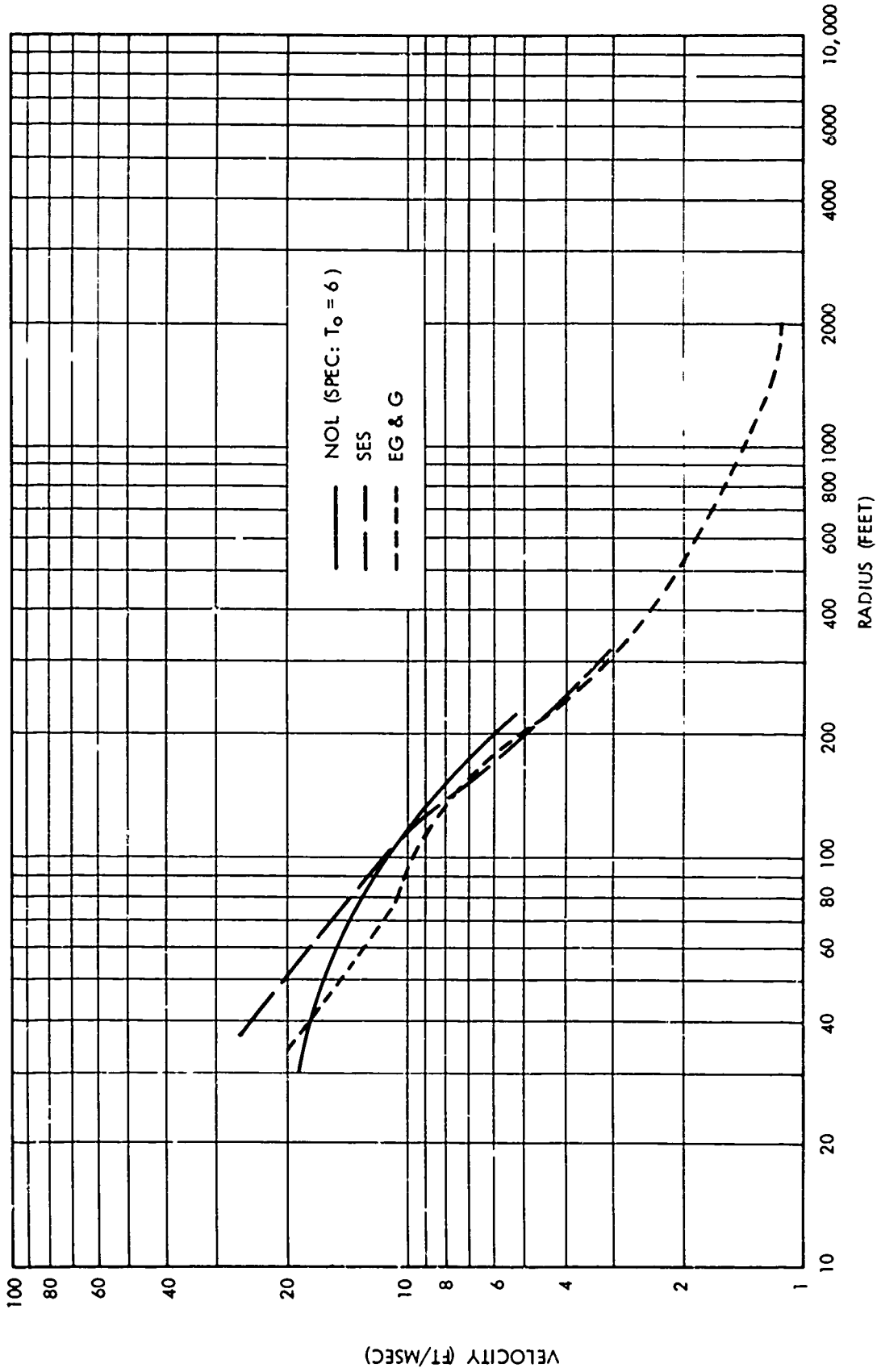


FIG. 14 SNOW BALL VELOCITY - DISTANCE CURVES

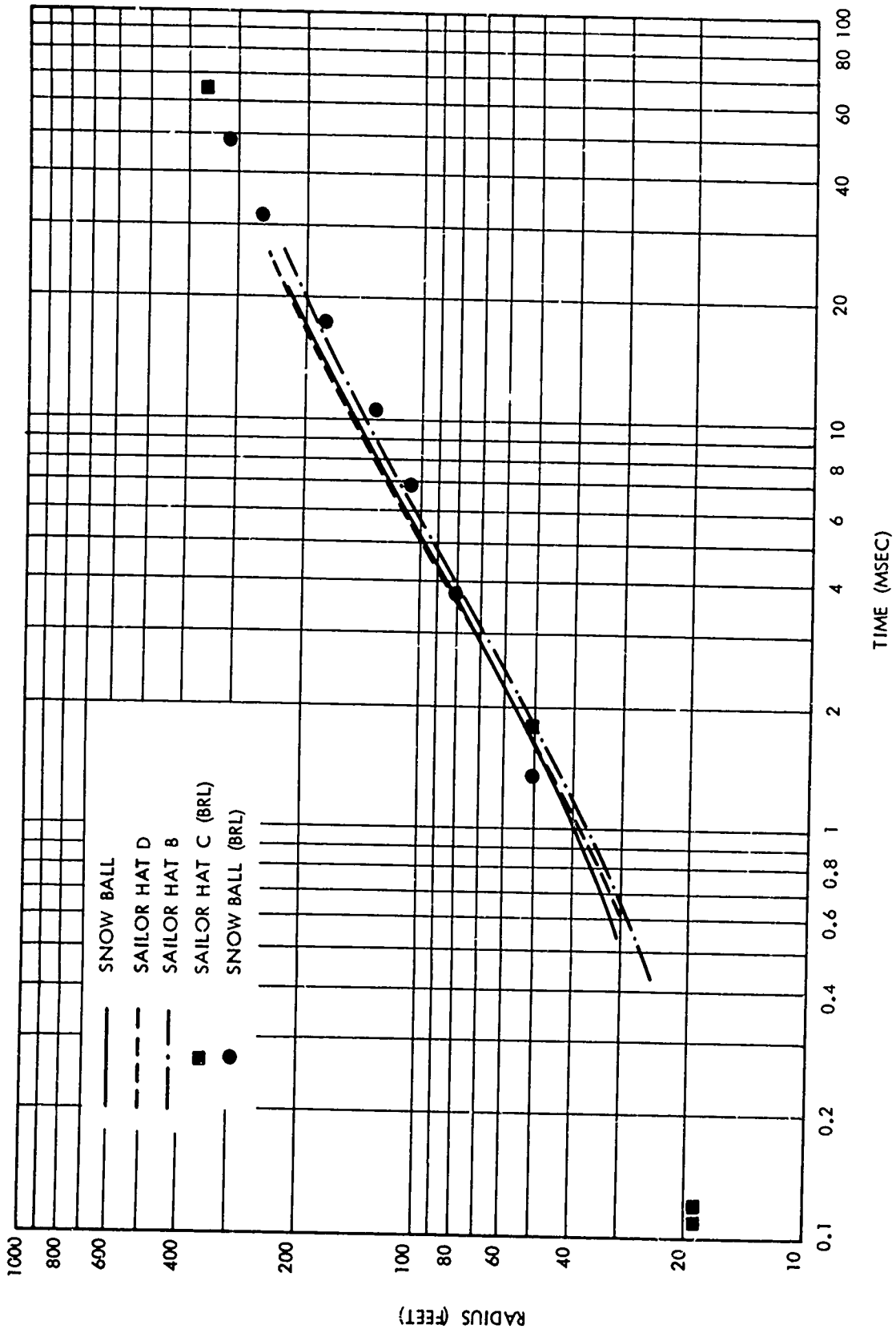


FIG. 15 500-TON HEMISPHERE RADIUS-TIME CURVES
(SPEC: $T_0 = 6$)

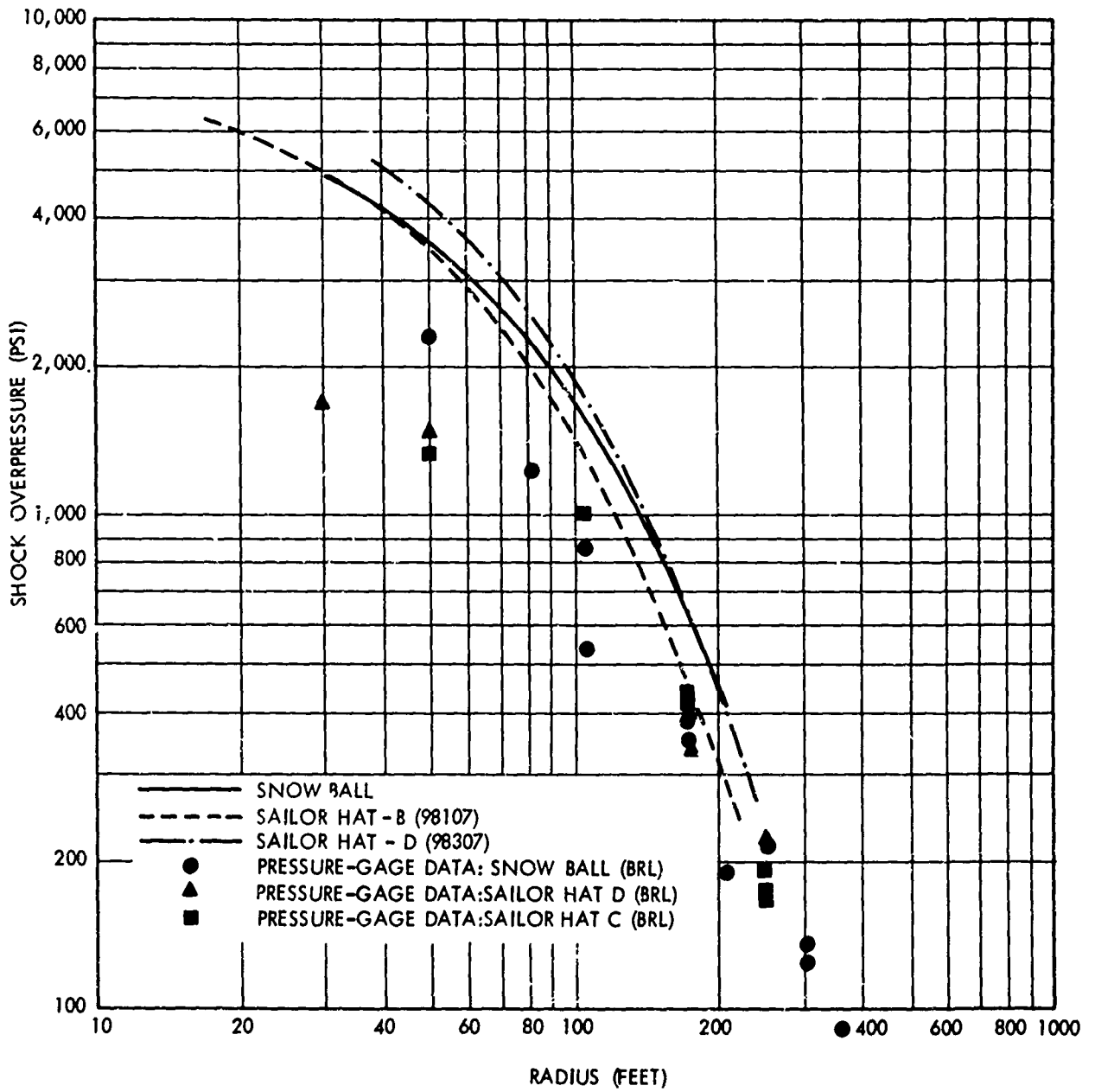


FIG. 16 500-TON TNT HEMISPHERE PRESSURE - DISTANCE CURVES
(SPEC: $T_0 = 6$)

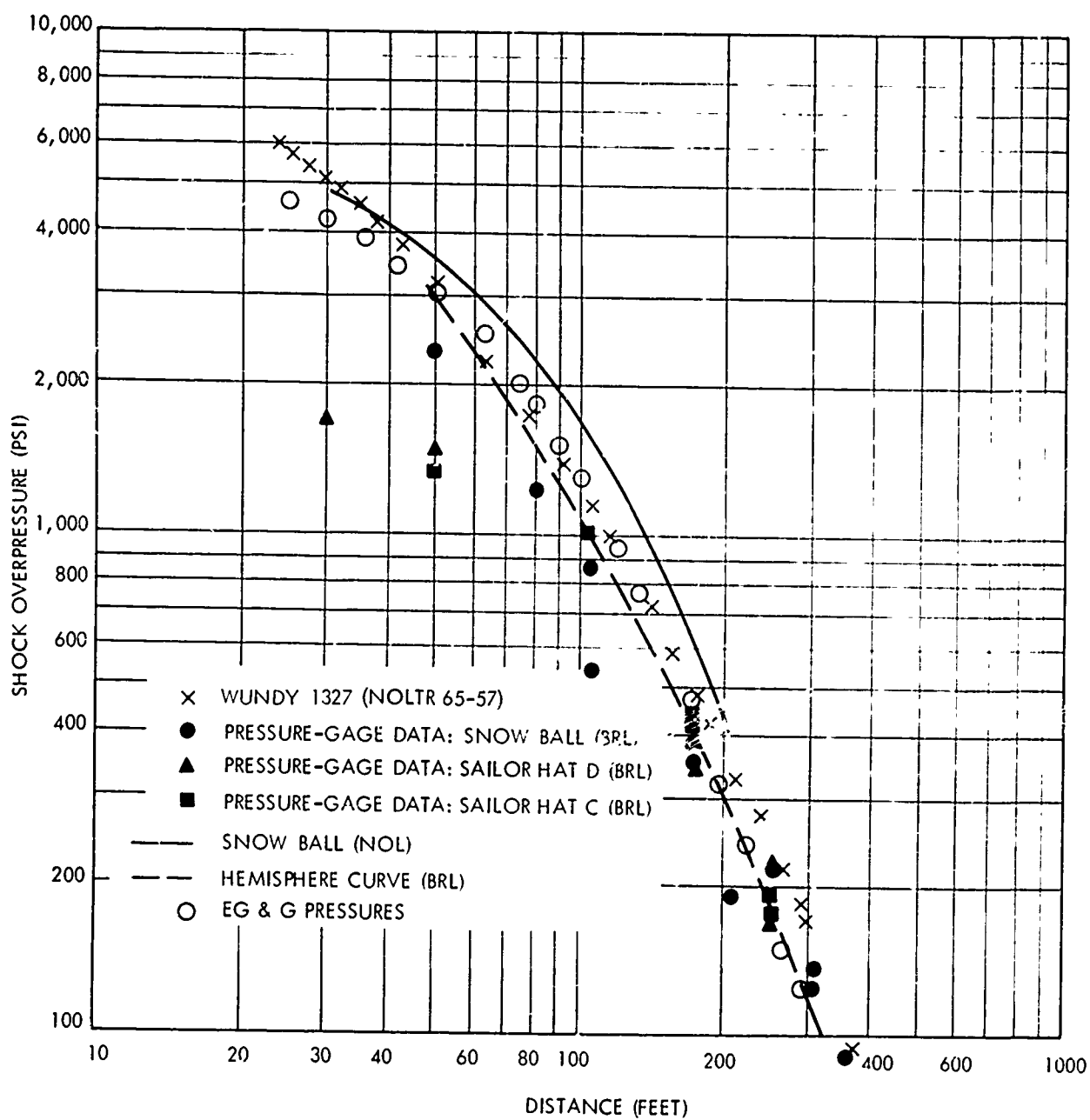


FIG. 17 COMPARISON OF AIRBLAST PRESSURES FROM VARIOUS MULTITON CHARGES WITH COMPUTED VALUES

APPENDIX 1

Procedure Used for Computing Pressure-Distance Curves from Rad' -Time Data.

1.1 INTRODUCTION:

A detailed discussion of a computational method for finding pressure-distance curves that we have repeatedly used in the past for small-sphere explosions has been given by Lehto and Belliveau.* A number of difficulties arose in application of this method to the SNOW BALL radius-time data and a new computational method, RFIT, had to be developed. A detailed discussion has been given by Connor.** In this Appendix we summarize the basic procedure and the application to our film data from SNOW BALL and SAILOR HAT.

Shock radius is measured on the film in arbitrary units as a function of frame number; appropriate scale factors then are used to convert these numbers to real time and distance.

Next we evaluate the parameters in an analytic function to fit radius-time measurements: $R = f(t)$, where $f(t)$ is a single-valued function of time. The time derivative of this function can then be obtained to give shock velocity as a function of time. The shock overpressures can then be found from the computed velocity values through use of the Rankine-Hugoniot relations, as given by Lehto and Belliveau, between shock overpressure and shock velocity.

1.2 RADIUS-TIME FITTING:

Radius-time data points can be least-squares fitted to any desired degree of accuracy by a variety of functions. However, the range of possible choices is narrowed considerably by the requirement that the fit be smoothly monotonically increasing.

Smoothness is a necessary restriction, since we ultimately use the time derivative of the fit for calculations of airshock pressure which we expect to

* D. L. Lehto and L. J. Belliveau, "The Treatment of Airblast Radius-Time and Pressure-Distance Data by the Use of Polynomial Approximations, with Applications to Pentolite Data," NOLTR 62-85, July 1963.

** J. G. Connor, Jr., "RFIT: Computer Analysis of High-Speed Explosion Photographs," Internal Memorandum, U. S. Naval Ordnance Laboratory, 6 June 1966.

decay smoothly. If the R-t curve is required to pass arbitrarily close to every data point it will meander from point to point and the derivative will fluctuate rather wildly, leading to computed pressures that are physically meaningless. We want, therefore, to represent the physical explosion growth correctly but not necessarily to connect every radius-time value available.

In the past variable-order polynomial functions have performed satisfactorily for fitting R-t data from small spherical explosions. These data were obtained from direct photography of the shock motion made visible by using a light refraction technique, in the low-pressure region, say from 100 to 1 psi. All our 500-ton data, on the other hand, come from indirect shock motion* in the high-pressure region above 100 psi. Our application of the polynomial functions to the 500-ton data led to fluctuating pressures of doubtful meaning.

We, therefore, have used a new function that behaves satisfactorily for both 500-ton charges and for small charges, SPEC, defined by

$$R = C_0 (t + T_0) + C_1 + C_2 \ln (t + T_0) + \frac{C_3}{t + T_0}$$

where C_0 = ambient sound speed; and C_1 , C_2 and C_3 are the fitting parameters. T_0 is an adjustable constant which must be determined. T_0 has the effect of moving the origin on the time axis away from the data. This is desirable because the last two terms in the function diverge rapidly to infinity at different rates when the value of their argument approaches zero. Adding T_0 prevents these arguments from approaching zero in the range over which the fitting is carried out, thus avoiding the appearance of a "hook" which appears in the fitted curve at early times if $T_0 = 0$.

SPEC has two attractive properties: (1) it is always smooth; that is, it does not have the undulations characteristic of the variable-order polynomials at the ends of the fitted regions; and (2) it grows rapidly at early times, more slowly at later times, qualitatively reproducing the shock behavior in time.

* All 500-ton film measurements have been made of the motion of the luminous front produced by the explosion. We, thus, assume that the shockfront and the luminous front are essentially identical.

1.3 EVALUATION OF SPEC ON SMALL-CHARGE DATA:

In order to evaluate the behavior of SPEC and also to gain experience in adjusting the arbitrary constant T_0 , we applied SPEC to the collection of small-charge data compiled by Goodman.* This compilation contains both radius-time measurements from photography and pressure-distance measurements from gages.

We fitted the radius-time data from Goodman with SPEC and then computed pressures, which values could be then compared with Goodman's measured pressures. T_0 was given a fixed, but arbitrary value, for each fitting; a variety of T_0 values was used.

For the smooth set of Goodman data, SPEC has trouble fitting points only at early times. This is because of the opposing divergences of the logarithm and reciprocal terms in the function; at later times the function is necessarily smooth. Figure 1-1 shows the Goodman pressure-distance curve as a solid line, together with a family of pressure curves resulting from variations in T_0 . When $T_0 = 0$, agreement is fair in the middle- and low-pressure range; but the calculated pressures are orders of magnitude too large at 20 charge radii and closer. For $T_0 = 0.01$ the hook in the R-t fit produces negative pressures close to the charge. For larger T_0 (i.e., 2 and 8) the shape of the calculated pressure curve is totally unacceptable.

The best match to the measured pressures in the fits shown in Figure 1-1 was obtained for $T_0 = 0.07$. The average per cent deviation of the fit from the data for radius-time is 0.2 per cent smaller for $T_0 = 0.07$ than for $T_0 = 0.05$ or 0.085. We noticed a correlation between the average per cent deviation of the fitted R-t curve from the R-t data points and the precision of the pressures derived from it. For the Goodman data a minimum average per cent deviation in R-t data coincided with the best overall reproduction of the pressure-distance curve.

SPEC pressures are sensitive to the precise numerical values of all R-t data used and various tests were made to obtain clarification of the interplay between the experimental R-t data input and the SPEC-pressure output. One of these tests is illustrated in Figure 1-2. For this test, we selected out of the full set of R-t data, drawn as the Goodman curve in Figure 1-1, only data over the range of $R = 1.5$ to $14 a_0$. This range corresponded to the range of R for which we had

* H. J. Goodman, "Compiled Free-Air Blast Data on Bare Spherical Pentolite," BRL Report No. 1092, February 1960.

SNOW BALL data. This selected set of R-t data was then processed by SPEC for the three values of $T_0 = 0.06, 0.6, \text{ and } 6$. We note that the SPEC results for $T_0 = 0.06$ in Figure 1-2 and for $T_0 = 0.07$ in Figure 1-1 differ only slightly and surmise that SPEC with a T_0 value of about 0.06 will provide a reasonably good fit to small-charge free-air data.

1.4 APPLICATION OF SPEC TO 500-TON DATA:

We do not have comparable pressure-gage data for the 500-ton explosions to guide us in creating an arbitrary fitting function as we had for small charges. We have no basis for directly applying the SPEC function that we evaluated from Goodman's data to the 500-ton data - the charges are of different explosive, different construction, different symmetry, and fired under different conditions. Nevertheless, we must find some suitable way of fitting the 500-ton data. And since the correct physical dependence of R as $f(t)$ is unknown to us, an arbitrary function, like SPEC, is as good as any other function for examination.

We have, therefore, applied SPEC to the SNOW BALL data with $T_0 = 6$ (the $T_0 = 0.06$ value scaled up by 100 for 500-ton hemispheres). Since we could not be sure how sensitively the SNOW BALL fits depended on the T_0 value, we made a number of runs with a range of T_0 values, as plotted in Figure 1-3. The y-axis in this figure represents the average deviation of computed R-values from experimental R-values at fixed times in a single fit with a fixed value of T_0 . We note that the average deviation is not especially sensitive to T_0 and that a value $T_0 = 6$ is appropriate.

We have no way of confirming that the SNOW BALL pressures that we compute with SPEC ($T_0 = 6$) are correct. We can only assume that, since the best pressure fit to the small-charge pressures occurred for a minimum value of average deviation in R-t, a similar best fit in pressures will occur for the minimum deviation in R-t for the 500-ton data. Additional checks on the derived pressures for SNOW BALL are discussed in the text of this report.

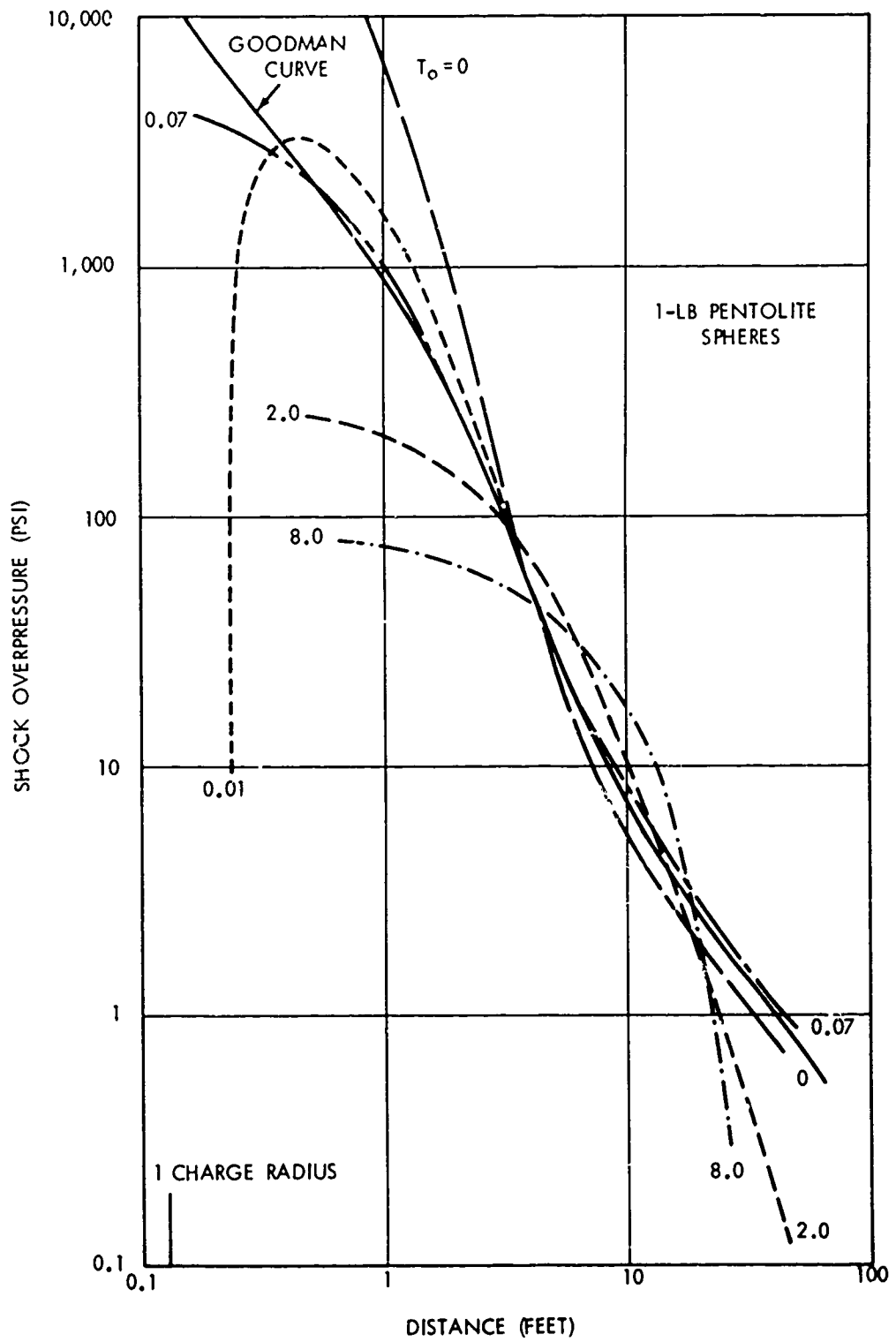


FIG. 1-1 COMPARISON OF SPEC P-R CURVES WITH SMALL CHARGE CURVE

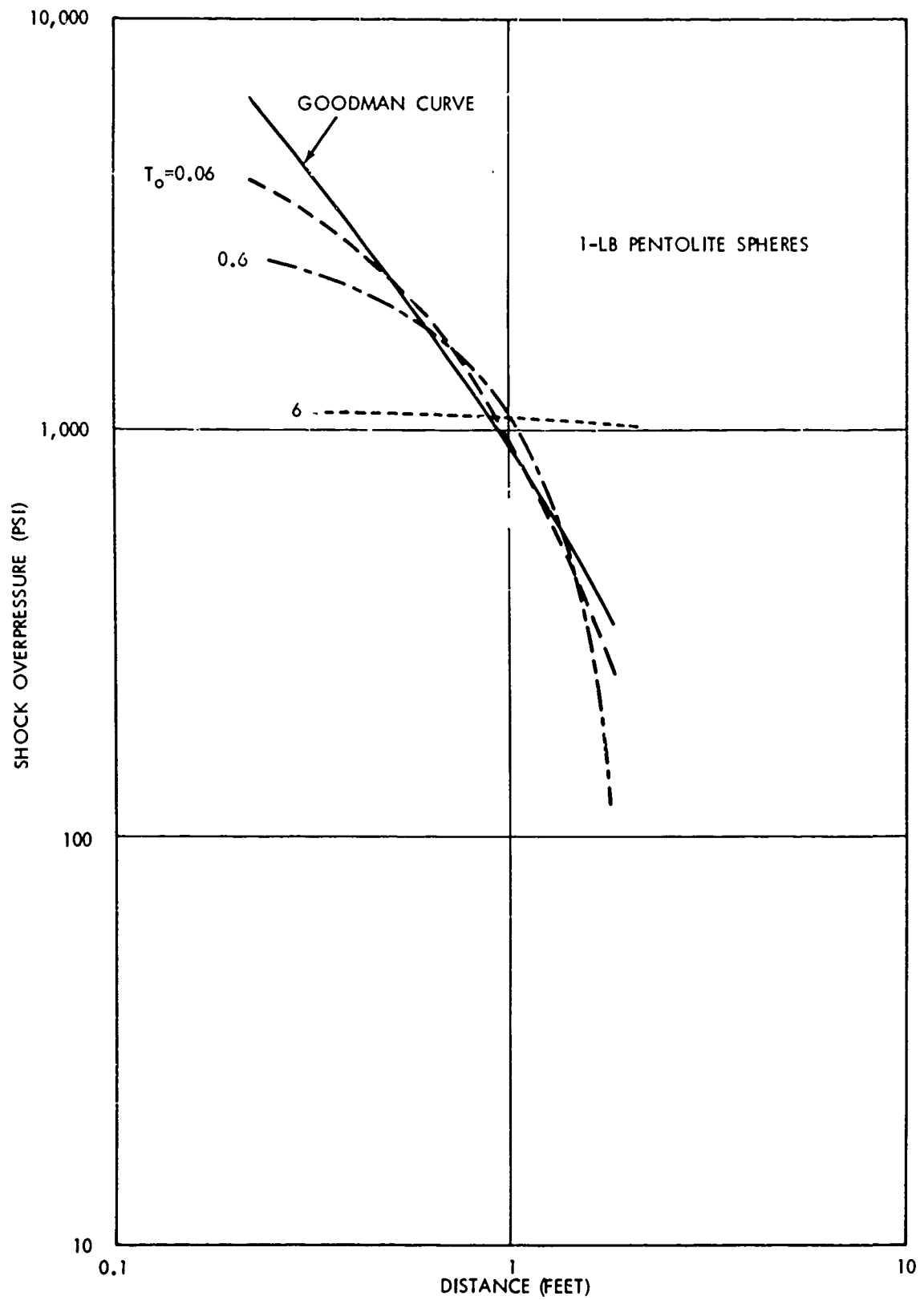


FIG. 1-2 COMPARISON OF SPEC P-R CURVES WITH SMALL CHARGE CURVE FROM $R \sim 1.5$ TO 14 CHARGE RADII

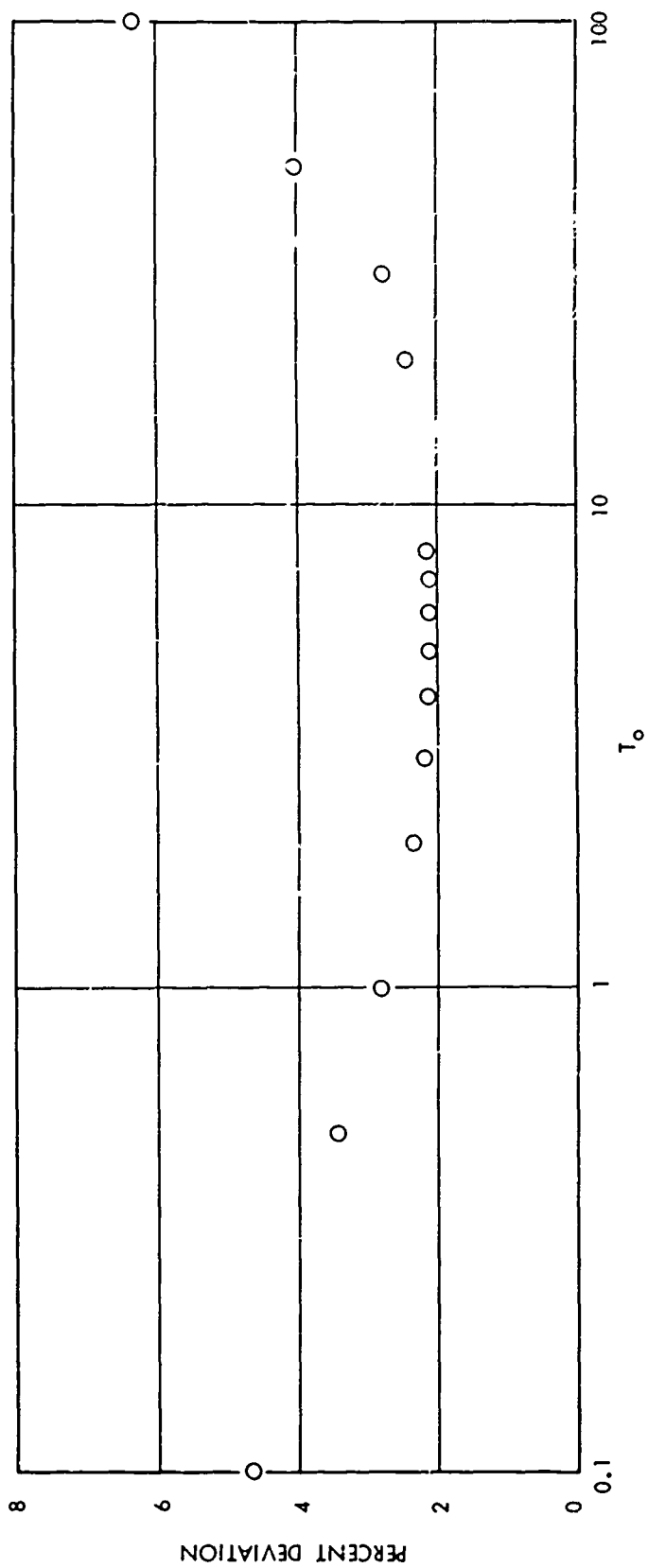


FIG. 1-3 AVERAGE DEVIATIONS IN SPEC FITS TO SNOW BALL RADIUS-TIME DATA

APPENDIX 2

Corrections for Time in Radius-Time Data

A detailed discussion of the procedure used for making measurements of radius-time growth from films (using a Telereadex machine) has been given by Connor.* We note here briefly only the procedure used to correct for time in the reduction of the 500-ton data processed for this report.

Time corrections are vital in the data-processing program because the least-squares fitting program in the data-processing procedure gives undue importance to the earliest frames in a film. In a typical millisecond-camera film, we can establish the first frame after explosion because this frame contains the first brilliant image, denoting explosion of the charge. Zero time (first appearance of explosion light) has occurred either during the dead time between the first and the zeroth frame, or, possibly, during the writing time for the first frame. Since the explosion luminosity grows rapidly with time during the earliest times, the fixed time uncertainties are relatively much more important for the early frames than for late frames, during which the explosion grows slowly.

A data-fitting procedure, in fitting a function to all R-t data, will vary the fitted function at late times to accommodate the R-t values at early times. Since there are fewer frames at early times and the time uncertainties are largest (relatively) for these frames, time corrections must be made and an appropriate computational procedure followed.

The 500-ton films were processed as follows. Seven rays from the hemisphere center were followed from frame to frame, a set of distances along a ray in each frame composing a set of input data for that ray. From these data from the seven rays the computer finds the nearest two distances along a ray to the edge of the original charge and fits a straight line to these nearest two points in the R-t plane, defining the time $t = 0$ when $R = la_0$, where a_0 is the charge radius. The time scale is then assigned and used for all R-t values along that ray. Thus, a given frame provides seven separate, independent values of R and t. From n frames the computer will fit a function to all seven n values of R and of t.

* J. G. Connor, Jr., "RFIT: Computer Analysis of High-Speed Explosion Photographs," Internal Memorandum, U. S. Naval Ordnance Laboratory, 6 June 1966.

NOLTR 67-94

Figure 2-1 illustrates some of the detailed results from our SNOW BALL film. The solid line is the resultant SPEC curve for the film. The data symbols are the R-t values, time corrected to $R = la_0$. The scatter in the early frames is somewhat exaggerated by the logarithmic plot. Not all seven symbols can be seen for each frame, since R-t values were occasionally identical.

Another time problem can arise in cutting off radius-time data when the airshock separates from the luminous front - at a relatively late time when the luminous front has nearly reached its maximum distance. In some films, the non-luminous airshock can be followed after separation, either by natural or intentionally-employed refracting effects. More typically, in explosion films the airshock is not visible; and the continuing, but much slower, growth of the luminous front after separation does not represent the R-t motion of the shock.

This cut-off problem did not arise in the 500-ton films considered in this report. The luminous-front edge of SNOW BALL moved out of the frame, cutting off R-t data, at a time well before separation.* Our corresponding SAILOR HAT data were taken only over the SNOW BALL range of R-t data.

* HANSEN (see references) has reported this separation time from EG&G films to be ~ 43 millisecc for SNOW BALL, well beyond our frame cut-off time of about 25 millisecc.

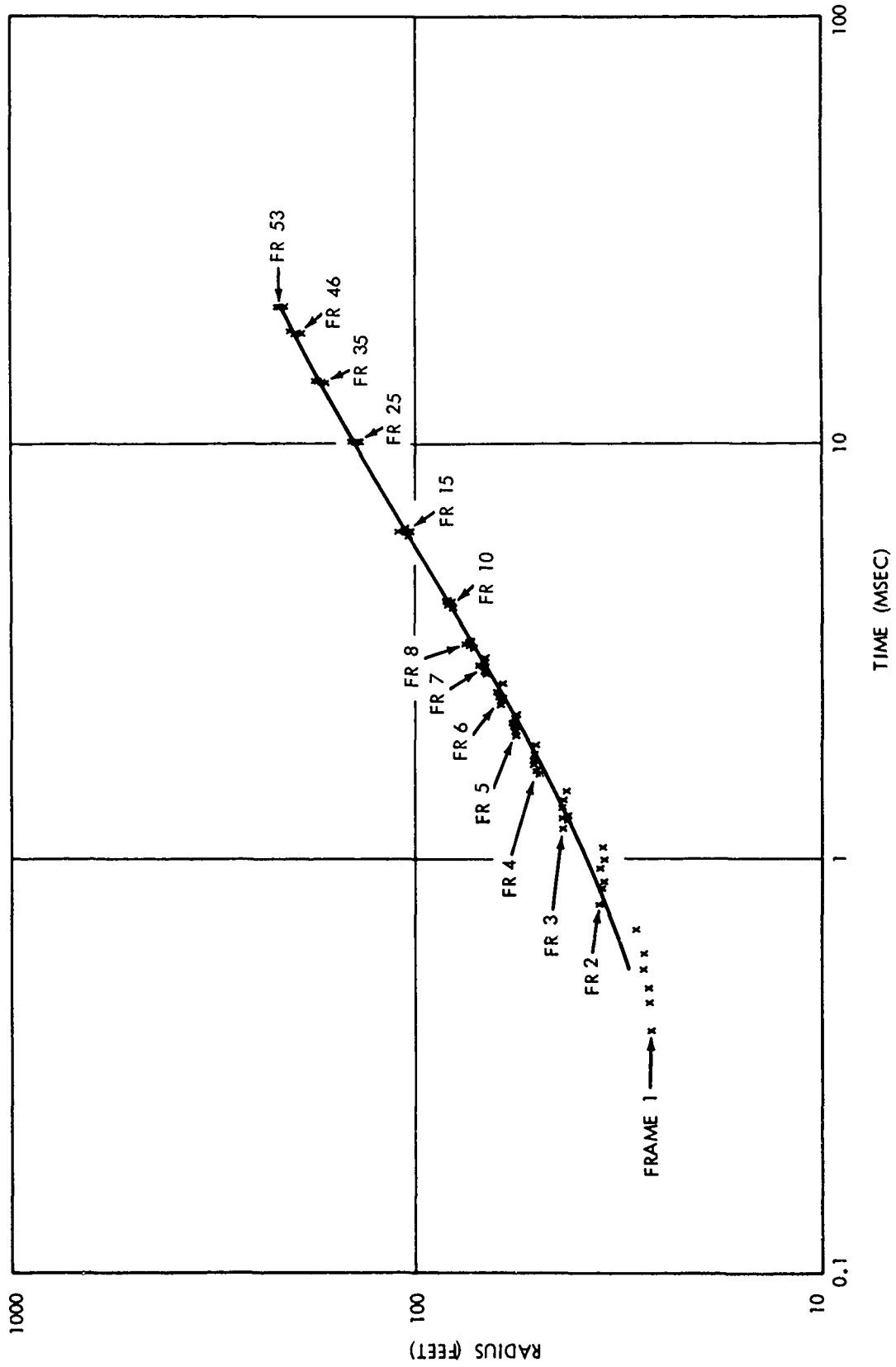


FIG. 2-1 COMPARISON OF FITTED SPEC CURVE WITH FILM DATA
(SNOW BALL XR FILM)

UNCLASSIFIED

Security Classification

DOCUMENT CONTROL DATA - R&D		
<i>(Security classification of title, body of abstract and indexing annotation must be entered when the overall report is classified)</i>		
1 ORIGINATING ACTIVITY (Corporate author) U. S. Naval Ordnance Laboratory White Oak, Silver Spring, Maryland 20910		2a REPORT SECURITY CLASSIFICATION UNCLASSIFIED
		2b GROUP
3 REPORT TITLE THE EARLY OPTICAL SPECTRUM AND AIRSHOCK FROM A 500-TON TNT EXPLOSION (Proj. 1.14 of Operation SNOW BALL)		
4 DESCRIPTIVE NOTES (Type of report and inclusive dates)		
5 AUTHOR(S) (Last name, first name, initial) Rudlin, L., Connor, J. G., Jr., and Wisotski, John		
6. REPORT DATE 5 October 1967	7a. TOTAL NO. OF PAGES 67	7b. NO. OF REFS 11
8a. CONTRACT OR GRANT NO.	9a. ORIGINATOR'S REPORT NUMBER(S) NOLTR 67-94	
b. PROJECT NO. NWER Subtask 01.002		
c. NOL-907	9b. OTHER REPORT NO(S) (Any other numbers that may be assigned this report)	
d.		
10. AVAILABILITY/LIMITATION NOTICES		
11. SUPPLEMENTARY NOTES	12 SPONSORING MILITARY ACTIVITY Defense Atomic Support Agency	
13. ABSTRACT Three photographic records were obtained by Project 1.14 on SNOW BALL: two millisecond framing-camera films of the explosion and one streak film of the optical spectrum. From these records (and others from small charges) we have: (1) deduced that the explosion light was produced largely by impurity radiation - from sodium, calcium, and cyanogen - and by forbidden O ₂ -bands; expected airshock radiation was not detected; (2) derived airshock pressures in the region, roughly, 5000 to 200 psi. These derived pressures are about a factor of 2 higher than pressure-gage values. Possible explanations for this discrepancy are discussed - including the possibility that the airshock and the luminosity front were not well coupled - but no satisfactory explanation has been found.		

DD FORM 1473
1 JAN 64

UNCLASSIFIED

Security Classification

14 KEY WORDS	LINK A		LINK B		LINK C	
	ROLE	WT	ROLE	WT	ROLE	WT
Operation SNOW BALL " SAILOR HAT Shockwaves (Chemical Explosion) Explosion Spectra TNT Pressure-Distance Surface Explosions Fireball Motion (Chem. Exp.)						

INSTRUCTIONS

1. **ORIGINATING ACTIVITY.** Enter the name and address of the contractor, subcontractor, grantee, Department of Defense activity or other organization (*corporate author*) issuing the report.
- 2a. **REPORT SECURITY CLASSIFICATION:** Enter the overall security classification of the report. Indicate whether "Restricted Data" is included. Marking is to be in accordance with appropriate security regulations.
- 2b. **GROUP:** Automatic downgrading is specified in DoD Directive 5200.10 and Armed Forces Industrial Manual. Enter the group number. Also, when applicable, show that optional markings have been used for Group 3 and Group 4 as authorized.
3. **REPORT TITLE:** Enter the complete report title in all capital letters. Titles in all cases should be unclassified. If a meaningful title cannot be selected without classification, show title classification in all capitals in parenthesis immediately following the title.
4. **DESCRIPTIVE NOTES:** If appropriate, enter the type of report, e.g., interim, progress, summary, annual, or final. Give the inclusive dates when a specific reporting period is covered.
5. **AUTHOR(S):** Enter the name(s) of author(s) as shown on or in the report. Enter last name, first name, middle initial. If military, show rank and branch of service. The name of the principal author is an absolute minimum requirement.
6. **REPORT DATE.** Enter the date of the report as day, month, year; or month, year. If more than one date appears on the report, use date of publication.
- 7a. **TOTAL NUMBER OF PAGES:** The total page count should follow normal pagination procedures, i.e., enter the number of pages containing information.
- 7b. **NUMBER OF REFERENCES:** Enter the total number of references cited in the report.
- 8a. **CONTRACT OR GRANT NUMBER.** If appropriate, enter the applicable number of the contract or grant under which the report was written.
- 8b, 8c, & 8d. **PROJECT NUMBER:** Enter the appropriate military department identification, such as project number, subproject number, system numbers, task number, etc.
- 9a. **ORIGINATOR'S REPORT NUMBER(S):** Enter the official report number by which the document will be identified and controlled by the originating activity. This number must be unique to this report.
- 9b. **OTHER REPORT NUMBER(S):** If the report has been assigned any other report numbers (*either by the originator or by the sponsor*), also enter this number(s).
10. **AVAILABILITY/LIMITATION NOTICES:** Enter any limitations on further dissemination of the report, other than those

imposed by security classification, using standard statements such as:

- (1) "Qualified requesters may obtain copies of this report from DDC."
- (2) "Foreign announcement and dissemination of this report by DDC is not authorized."
- (3) "U. S. Government agencies may obtain copies of this report directly from DDC. Other qualified DDC users shall request through _____."
- (4) "U. S. military agencies may obtain copies of this report directly from DDC. Other qualified users shall request through _____."
- (5) "All distribution of this report is controlled. Qualified DDC users shall request through _____."

If the report has been furnished to the Office of Technical Services, Department of Commerce, for sale to the public, indicate this fact and enter the price, if known.

11. **SUPPLEMENTARY NOTES:** Use for additional explanatory notes.
12. **SPONSORING MILITARY ACTIVITY:** Enter the name of the departmental project office or laboratory sponsoring (*paying for*) the research and development. Include address.
13. **ABSTRACT:** Enter an abstract giving a brief and factual summary of the document indicative of the report, even though it may also appear elsewhere in the body of the technical report. If additional space is required, a continuation sheet shall be attached.

It is highly desirable that the abstract of classified reports be unclassified. Each paragraph of the abstract shall end with an indication of the military security classification of the information in the paragraph, represented as (TS) (S) (C) or (U)

There is no limitation on the length of the abstract. However, the suggested length is from 150 to 225 words.

14. **KEY WORDS:** Key words are technically meaningful terms or short phrases that characterize a report and may be used as index entries for cataloging the report. Key words must be selected so that no security classification is required. Identifiers, such as equipment model designation, trade name, military project code name, geographic location, may be used as key words but will be followed by an indication of technical context. The assignment of links, roles, and weights is optional.

1.5 662 4.4

UNCLASSIFIED

U.S. NAVAL ORDNANCE LABORATORY
WHITE OAK
SILVER SPRING, MARYLAND 20910



To all holders of NOLTR 67-94
Title: **The Early Optical Spectrum and Airshock From
a 500-ton TNT Explosion**

Change 1
29 Feb 1968

Approved by Commander, U.S. NOL

(Signature)
By direction

1 page

This publication is changed as follows:

Page 20, line 5 from bottom: Change 225 millisec to 300 millisec.

Comment: The authors are indebted to Mr. J. D. R. Pattman of the Defence Chemical, Biological and Radiation Laboratories, Ottawa, for pointing out our error. This 300 millisec value for second-shock brightening now agrees satisfactorily with the 285 millisec value found on the NOL film. Neither value, however, agrees with the comparable EG&G time of 230 millisec. This situation, probably, reinforces the guess, page 21, that the explosion phenomena differed on the U. S. and the Canadian views of the SNOW BALL explosion.

Insert this change sheet between the cover and the title page of your copy.
Write on cover "Change 1 inserted"

UNCLASSIFIED